Hydrol. Earth Syst. Sci., 20, 4775–4799, 2016
www.hydrol-earth-syst-sci.net/20/4775/2016/
doi:10.5194/hess-20-4775-2016

Hydrology and Earth System Sciences
Open Access
EGU

The evolution of root-zone moisture capacities after deforestation: a step towards hydrological predictions under change?

Remko Nijzink[1], Christopher Hutton[2], Ilias Pechlivanidis[4], René Capell[4], Berit Arheimer[4], Jim Freer[2,3], Dawei Han[2], Thorsten Wagener[2,3], Kevin McGuire[5], Hubert Savenije[1], and Markus Hrachowitz[1]

[1]Water Resources Section, Faculty of Civil Engineering and Geosciences, Delft University of Technology, Stevinweg 1, 2628 CN Delft, the Netherlands
[2]Department of Civil Engineering, University of Bristol, Bristol, UK
[3]Cabot Institute, University of Bristol, Bristol, UK
[4]Swedish Meteorological and Hydrological Institute (SMHI), Norrköping, Sweden
[5]Virginia Water Resources Research Center and Department of Forest Resources and Environmental Conservation, Virginia Tech, Blacksburg, VA, USA

Correspondence to: Remko Nijzink (r.c.nijzink@tudelft.nl)

Received: 21 August 2016 – Published in Hydrol. Earth Syst. Sci. Discuss.: 29 August 2016
Revised: 5 November 2016 – Accepted: 11 November 2016 – Published: 5 December 2016

Abstract. The core component of many hydrological systems, the moisture storage capacity available to vegetation, is impossible to observe directly at the catchment scale and is typically treated as a calibration parameter or obtained from a priori available soil characteristics combined with estimates of rooting depth. Often this parameter is considered to remain constant in time. Using long-term data (30–40 years) from three experimental catchments that underwent significant land cover change, we tested the hypotheses that: (1) the root-zone storage capacity significantly changes after deforestation, (2) changes in the root-zone storage capacity can to a large extent explain post-treatment changes to the hydrological regimes and that (3) a time-dynamic formulation of the root-zone storage can improve the performance of a hydrological model.

A recently introduced method to estimate catchment-scale root-zone storage capacities based on climate data (i.e. observed rainfall and an estimate of transpiration) was used to reproduce the temporal evolution of root-zone storage capacity under change. Briefly, the maximum deficit that arises from the difference between cumulative daily precipitation and transpiration can be considered as a proxy for root-zone storage capacity. This value was compared to the value obtained from four different conceptual hydrological models that were calibrated for consecutive 2-year windows.

It was found that water-balance-derived root-zone storage capacities were similar to the values obtained from calibration of the hydrological models. A sharp decline in root-zone storage capacity was observed after deforestation, followed by a gradual recovery, for two of the three catchments. Trend analysis suggested hydrological recovery periods between 5 and 13 years after deforestation. In a proof-of-concept analysis, one of the hydrological models was adapted to allow dynamically changing root-zone storage capacities, following the observed changes due to deforestation. Although the overall performance of the modified model did not considerably change, in 51 % of all the evaluated hydrological signatures, considering all three catchments, improvements were observed when adding a time-variant representation of the root-zone storage to the model.

In summary, it is shown that root-zone moisture storage capacities can be highly affected by deforestation and climatic influences and that a simple method exclusively based on climate data can not only provide robust, catchment-scale estimates of this critical parameter, but also reflect its time-dynamic behaviour after deforestation.

Published by Copernicus Publications on behalf of the European Geosciences Union.

1 Introduction

Vegetation, as a core component of the water cycle, shapes the partitioning of water fluxes on the catchment scale into runoff components and evaporation, thereby controlling fundamental processes in ecosystem functioning (Rodriguez-Iturbe, 2000; Laio et al., 2001; Kleidon, 2004), such as flood generation (Donohue et al., 2012), drought dynamics (Seneviratne et al., 2010; Teuling et al., 2013), groundwater recharge (Allison et al., 1990; Jobbágy and Jackson, 2004) and land–atmosphere feedback (Milly and Dunne, 1994; Seneviratne et al., 2013; Cassiani et al., 2015). Besides increasing interception storage available for evaporation (Gerrits et al., 2010), vegetation critically interacts with the hydrological system in a co-evolutionary way by root water uptake for transpiration, towards a dynamic equilibrium with the available soil moisture to avoid water shortage (Donohue et al., 2007; Eagleson, 1978, 1982; Gentine et al., 2012; Liancourt et al., 2012) and related adverse effects on carbon exchange and assimilation rates (Porporato et al., 2004; Seneviratne et al., 2010). Roots create moisture storage volumes within their range of influence, from which they extract water that is stored between field capacity and wilting point. This root-zone storage capacity S_R, sometimes also referred to as plant available water holding capacity, in the unsaturated soil is therefore the key component of many hydrological systems (Milly and Dunne, 1994; Rodriguez-Iturbe et al., 2007).

There is increasing theoretical and experimental evidence that vegetation dynamically adapts its root system, and thus S_R, to environmental conditions, to secure, on the one hand, access to sufficient moisture to meet the canopy water demand and, on the other hand, to minimize the carbon investment for sub-surface growth and maintenance of the root system (Brunner et al., 2015; Schymanski et al., 2008; Tron et al., 2015). In other words, the hydrologically active root zone is optimized to guarantee productivity and transpiration of vegetation, given the climatic circumstances (Kleidon, 2004). Several studies previously showed the strong influence of climate on this hydrologically active root zone (e.g. Reynolds et al., 2000; Laio et al., 2001; Schenk and Jackson, 2002). Moreover, droughts are often identified as critical situations that can affect ecosystem functioning evolution (e.g. Allen et al., 2010; McDowell et al., 2008; Vose et al., 2016).

In addition to their general adaption to environmental conditions, vegetation has some potential to adapt roots to such periods of water shortage (Sperry et al., 2002; Mencuccini, 2003; Bréda et al., 2006). In the short term, stomatal closure and reduction of leaf area will lead to reduced transpiration. In several case studies for specific plants, it was also shown that plants may even shrink their roots and reduce soil–root conductivity during droughts, while recovering after re-wetting (Nobel and Cui, 1992; North and Nobel, 1992). In the longer term, and more importantly, trees can improve their internal hydraulic system, for example by recovering damaged xylem or by allocating more biomass for roots (Sperry et al., 2002; Rood et al., 2003; Bréda et al., 2006). Similarly, Tron et al. (2015) argued that roots follow groundwater fluctuations, which may lead to increased rooting depths when water tables drop. Such changing environmental conditions may also provide other plant species with different water demand than the ones present under given conditions, with an advantage in the competition for resources, as for example shown by Li et al. (2007).

The hydrological functioning of catchments (Black, 1997; Wagener et al., 2007) and thus the partitioning of water into evaporative fluxes and runoff components is not only affected by the continuous adaption of vegetation to changing climatic conditions. Rather, it is well understood that anthropogenic changes to land cover, such as deforestation, can considerably alter hydrological regimes. This has been shown historically through many paired watershed studies (e.g. Bosch and Hewlett, 1982; Andréassian, 2004; Brown et al., 2005; Alila et al., 2009). These studies found that deforestation often leads to generally higher seasonal flows and/or an increased frequency of high flows in streams, while decreasing evaporative fluxes. The timescales of hydrological recovery after such land-cover disturbances were shown to be highly sensitive to climatic conditions and the growth dynamics of the regenerating species (e.g. Jones and Post, 2004; Brown et al., 2005).

Although land-use change effects on hydrological functioning are widely acknowledged, it is less well understood which parts of the hydrological system are affected in which way and over which timescales. As a consequence, most catchment-scale models were originally not developed to deal with such changes in the system, but rather for "stationary" conditions (Ehret et al., 2014). This is true for both top-down hydrological models, such as HBV (Bergström, 1992) or GR4J (Perrin et al., 2003), and bottom-up models, such as MIKE-SHE (Refsgaard and Storm, 1995) or HydroGeoSphere (Brunner and Simmons, 2012). Several modelling studies have in the past incorporated temporal effects of land-use change to some degree (Andersson and Arheimer, 2001; Bathurst et al., 2004; Brath et al., 2006), but they mostly rely on ad hoc assumptions about how hydrological parameters are affected (Legesse et al., 2003; Mahe et al., 2005; Onstad and Jamieson, 1970; Fenicia et al., 2009). Approaches which incorporate the change in the model formulation itself are rare and have only recently gained momentum (e.g. Du et al., 2016; Fatichi et al., 2016; Zhang et al., 2016). This is of critical importance as ongoing changes in land cover and climate dictate the need for a better understanding of their effects on hydrological functioning (Troch et al., 2015) and their explicit consideration in hydrological models for more reliable predictions under change (Hrachowitz et al., 2013; Montanari et al., 2013).

As a step towards such an improved understanding and the development of time-dynamic models, we argue that the

Table 1. Overview of the catchments and their sub-catchments (WS).

Catchment	Deforestation period	Treatment	Area [km^2]	Affected Area [%]	Aridity index [–]	Precipitation [mm yr^{-1}]	Discharge [mm yr^{-1}]	Potential evaporation [mm yr^{-1}]	Time series
HJ Andrews WS1	1962–1966	Burned 1966	0.956	100	0.39	2305	1361	902	1962–1990
HJ Andrews WS2	–	–	0.603	–	0.39	2305	1251	902	1962–1990
Hubbard Brook WS2	1965–1968	Herbicides	0.156	100	0.57	1471	1059	784	1961–2009
Hubbard Brook WS3	–	–	0.424	–	0.54	1464	951	787	1961–2009
Hubbard Brook WS5	1983–1984	No treatment	0.219	87	0.51	1518	993	746	1962–2009

root-zone storage capacity, S_R, is a core component determining the hydrological response, and needs to be treated as a dynamically evolving parameter in hydrological modelling as a function of climate and vegetation. Gao et al. (2014) recently demonstrated that catchment-scale S_R can be robustly estimated exclusively based on long-term water balance considerations. Wang-Erlandsson et al. (2016) derived global estimates of S_R using remote-sensing based precipitation and evaporation products, which demonstrated considerable spatial variability of S_R in response to climatic drivers. In traditional approaches, S_R is typically determined either by the calibration of a hydrological model (e.g. Seibert and McDonnell, 2010; Seibert et al., 2010) or based on soil characteristics and sparse, averaged estimates of root depths, often obtained from literature (e.g. Breuer et al., 2003; Ivanov et al., 2008). This does neither reflect the dynamic nature of the root system nor does it consider to a sufficient extent the actual function of the root zone: providing plants with continuous and efficient access to water. This leads to the situation where soil porosity often effectively controls the values of S_R used in a model. Consider, as a thought experiment, two plants of the same species growing on different soils. They will, with the same average root depth, then have access to different volumes of water, which will merely reflect the differences in soil porosity. This is in strong contradiction to the expectation that these plants would design root systems that provide access to similar water volumes, given the evidence for efficient carbon investment in root growth (Milly, 1994; Schymanski et al., 2008; Troch et al., 2009) and posing that plants of the same species have common limits of operation. This argument is supported by a recent study, in which was shown that water-balance-derived estimates of S_R are at least as plausible as soil-derived estimates (de Boer-Euser et al., 2016) in many environments and that the maximum root depth controls evaporative fluxes and drainage (Camporese et al., 2015).

Therefore, using water-balance-based estimates of S_R in several deforested sites as well as in untreated reference sites in two experimental forests, we test the hypotheses that (1) the root-zone storage capacity S_R significantly changes after deforestation, (2) the evolution in S_R can explain post-treatment changes to the hydrological regimes and that (3) a time-dynamic formulation of S_R can improve the performance of a hydrological model.

2 Study sites

The catchments under consideration are part of the HJ Andrews Experimental Forest and the Hubbard Brook Experimental Forest. A summary of the main catchment characteristics can be found in Table 1. Daily discharge (Campbell, 2014a; Johnson and Rothacher, 2016), precipitation (Campbell, 2014b; Daly and McKee, 2016) and temperature time series (Campbell, 2014c, d; Daly and McKee, 2016) were obtained from the databases of the Hubbard Brook Experimental Forest and the HJ Andrews Experimental Forest. Potential evaporation was estimated by the Hargreaves equation (Hargreaves and Samani, 1985).

2.1 HJ Andrews Experimental Forest

The HJ Andrews Experimental Forest is located in Oregon, USA (44.2° N, 122.2° W) and was established in 1948. The catchments at HJ Andrews are described in many studies (e.g. Rothacher, 1965; Dyrness, 1969; Harr et al., 1975; Jones and Grant, 1996; Waichler et al., 2005).

Before vegetation removal and at lower elevations the forest generally consisted of 100- to 500-year old coniferous species, such as Douglas fir (*Pseudotsuga menziesii*), western hemlock (*Tsuga heterophylla*) and western red cedar (*Thuja plicata*), whereas upper elevations were characterized by noble fir (*Abies procera*), Pacific silver fir (*Abies amabilis*), Douglas fir, and western hemlock. Most of the precipitation falls from November to April (about 80 % of the annual precipitation), whereas the summers are generally drier, leading to signals of precipitation and potential evaporation that are out of phase.

Deforestation of HJ Andrews Watershed 1 (WS1) started in August 1962 (Rothacher, 1970). Most of the timber was removed with skyline yarding. After finishing the logging in October 1966, the remaining debris was burned and the site was left for natural regrowth. Watershed 2 (WS2) is the reference catchment, which was not harvested.

2.2 Hubbard Brook Experimental Forest

The Hubbard Brook Experimental Forest is a research site established in 1955 and located in New Hampshire, USA (43.9° N, 71.8° W). The Hubbard Brook experimental catchments are described in a many publications (e.g. Hornbeck et al., 1970, 1997; Hornbeck, 1973; Dahlgren and Driscoll, 1994; Likens, 2013).

Prior to vegetation removal, the forest was dominated by northern hardwood forest composed of sugar maple (*Acer saccharum*), American beech (*Fagus grandifolia*) and yellow birch (*Betula alleghaniensis*) with conifer species such as red spruce (*Picea rubens*) and balsam fir (*Abies balsamea*) occurring at higher elevations and on steeper slopes with shallow soils. The forest was selectively harvested from 1870 to 1920, damaged by a hurricane in 1938, and is currently not accumulating biomass (Campbell et al., 2013; Likens, 2013). The annual precipitation and runoff is less than in HJ Andrews (Table 1). Precipitation is rather uniformly spread throughout the year without distinct dry and wet periods, but with snowmelt-dominated peak flows occurring around April and distinct low flows during the summer months due to increased evaporation rates (Federer et al., 1990). Vegetation removal occurred in the catchment of Hubbard Brook WS2 between 1965 and 1968 and in Hubbard Brook Watershed 5 (WS5) between 1983 and 1984. Hubbard Brook Watershed 3 (WS3) is the undisturbed reference catchment.

Hubbard Brook WS2 was completely deforested in November and December 1965 (Likens et al., 1970). To minimize disturbance, no roads were constructed and all timber was left in the catchment. On 23 June 1966, herbicides were sprayed from a helicopter to prevent regrowth. Additional herbicides were sprayed in the summers of 1967 and 1968 from the ground.

In Hubbard Brook WS5, all trees were removed between 18 October 1983 and 21 May 1984, except for a 2 ha buffer near an adjacent reference catchment (Hornbeck et al., 1997). WS5 was harvested as a whole-tree mechanical clearcut with removal of 93 % of the above-ground biomass (Hornbeck et al., 1997; Martin et al., 2000), thus including smaller branches and debris. Approximately 12 % of the catchment area was developed as the skid trail network. Afterwards, no treatment was applied and the site was left for regrowth.

3 Methodology

To assure reproducibility and repeatability, the executional steps in the experiment were defined in a detailed protocol, following Ceola et al. (2015), which is provided as Supplement Sect. S1.

Table 2. Applied parameter ranges for root-zone storage derivation.

Catchment	$I_{max,eq}$ (mm)	$I_{max,change}$ (mm)	T_r (days)
HJ Andrews WS1	1–5	0–5	0–3650
HJ Andrews WS2	1–5	–	–
Hubbard Brook WS2	1–5	5–10	0–3650
Hubbard Brook WS3	1–5	–	–
Hubbard Brook WS5	1–5	0–5	0–3650

3.1 Water-balance-derived root-zone moisture capacities S_R

The root-zone moisture storage capacities S_R and their change over time were determined according to the methods suggested by Gao et al. (2014) and subsequently successfully tested by de Boer-Euser et al. (2016) and Wang-Erlandsson et al. (2016). Briefly, the long-term water balance provides information on actual mean transpiration. In a first step, the interception capacity has to be assumed, in order to determine the effective precipitation P_e ($L\,T^{-1}$), following the water balance equation for interception storage:

$$\frac{dS_i}{dt} = P - E_i - P_e \tag{1}$$

with S_i (L) interception storage, P the precipitation ($L\,T^{-1}$), E_i the interception evaporation ($L\,T^{-1}$). This is solved with the constitutive relations:

$$E_i = \begin{cases} E_p & \text{if } E_p dt < S_i \\ \dfrac{S_i}{dt} & \text{if } E_p dt \geq S_i \end{cases} \tag{2}$$

$$P_e = \begin{cases} 0 & \text{if } S_i \leq I_{max} \\ \dfrac{S_i - I_{max}}{dt} & \text{if } S_i > I_{max} \end{cases} \tag{3}$$

with, additionally, E_p the potential evaporation ($L\,T^{-1}$) and I_{max} (L) the interception capacity. As I_{max} will also be affected by land cover change, this was addressed by introducing the three parameters $I_{max,eq}$ (long-term equilibrium interception capacity) (L), $I_{max,change}$ (post-treatment interception capacity) (L) and T_r (recovery time) (T), leading to a time-dynamic formulation of I_{max}:

$$I_{max} = \begin{cases} \text{for } t < t_{change}\,,\ t > t_{change,end} + T_r: \\ I_{max,eq} \\ \text{for } t_{change,start} < t < t_{change,end}: \\ I_{max,eq} - \dfrac{I_{max,eq} - I_{max,change}}{t_{change,end} - t_{change,start}} \left(t - t_{change,start}\right) \\ \text{for } t_{change,end} < t < t_{change,end} + T_r: \\ I_{max,change} + \dfrac{I_{max,eq} - I_{max,change}}{T_r} \left(t - t_{change,end}\right) \end{cases} \tag{4}$$

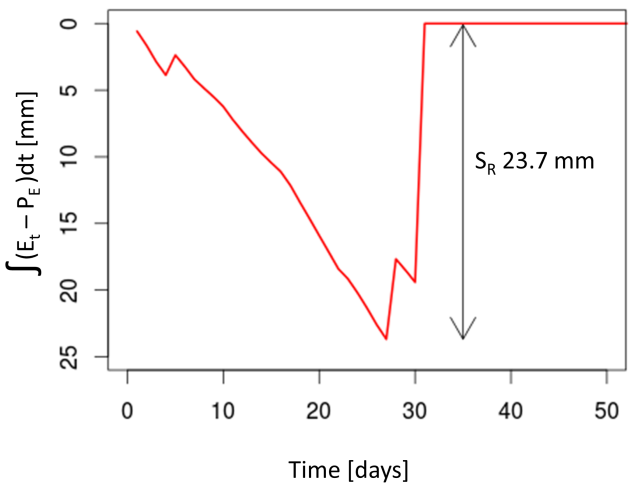

Figure 1. Derivation of root-zone storage capacity (S_R) for one specific time period in Hubbard Brook WS2 as difference between the cumulative transpiration (E_t) and the cumulative effective precipitation (P_E).

with $t_{change,start}$ the time that deforestation started and $t_{start,end}$ the time deforestation finished.

Following a Monte Carlo sampling approach, upper and lower bounds of E_i were then estimated based on 1000 random samples of these parameters, eventually leading to upper and lower bounds for P_e. The interception capacity was assumed to increase after deforestation for Hubbard Brook WS2, as the debris was left at the site. For Hubbard Brook WS5 and HJ Andrews WS1 the interception capacity was assumed to decrease after deforestation, as here the debris was respectively burned and removed. Furthermore, in the absence of more detailed information, it was assumed that the interception capacities changed linearly during deforestation towards $I_{max,change}$ and linearly recovered to I_{max} over the period T_r as well. See Table 2 for the applied parameter ranges.

Hereafter, the long-term mean transpiration can be estimated with the remaining components of the long term water balance, assuming no additional gains or losses, storage changes and/or data errors:

$$\overline{E_t} = \overline{P_e} - \overline{Q}, \tag{5}$$

where $\overline{E_t}$ ($L\,T^{-1}$) is the long-term mean actual transpiration, $\overline{P_e}$ ($L\,T^{-1}$) is the long-term mean effective precipitation and $\overline{Q}$ ($L\,T^{-1}$) is the long-term mean catchment runoff. Taking into account seasonality, the actual mean transpiration is scaled with the ratio of long-term mean daily potential evaporation E_p over the mean annual potential evaporation E_p:

$$E_t(t) = \frac{E_p(t)}{\overline{E_p}} \times \overline{E_t}. \tag{6}$$

Based on this, the cumulative deficit between actual transpiration and precipitation over time can be estimated by means of an "infinite-reservoir". In other words, the cumulative sum of daily water deficits, i.e. evaporation minus precipitation, is calculated between T_0, which is the time the deficit equals zero, and T_1, which is the time the total deficit returned to zero. The maximum deficit of this period then represents the volume of water that needs to be stored to provide vegetation continuous access to water throughout that time:

$$S_R = \max \int_{T0}^{T1} (E_t - P_e)\,dt, \tag{7}$$

where S_R (L) is the maximum root-zone storage capacity over the time period between T_0 and T_1. See also Fig. 1 for a graphical example of the calculation for the Hubbard Brook catchment for one specific realization of the parameter sampling. The $S_{R,20yr}$ for drought return periods of 20 years was estimated using the Gumbel extreme value distribution (Gumbel, 1941) as previous work suggested that vegetation designs S_R to satisfy deficits caused by dry periods with return periods of approximately 10–20 years (Gao et al., 2014; de Boer-Euser et al., 2016). Thus, the maximum values of S_R for each year, as obtained by Eq. (7), were fitted to the extreme value distribution of Gumbel, and subsequently, the $S_{R,20yr}$ was determined.

For the study catchments that experienced logging and subsequent reforestation, it was assumed that the root system converges towards a dynamic equilibrium approximately 10 years after reforestation. Thus, the equilibrium $S_{R,20yr}$ was estimated using only data over a period that started at least 10 years after the treatment. For the growing root systems during the years after reforesting, the storage capacity does not yet reach its dynamic equilibrium $S_{R,20yr}$. Instead of determining an equilibrium value, the maximum occurring deficit for each year was in that case considered as the maximum demand and thus as the maximum required storage $S_{R,1yr}$ for that year. To make these yearly estimates, the mean transpiration was determined in a similar way as stated by Eq. (5). However, the assumption of no storage change may not be valid for 1-year periods. In a trade-off to limit the potential bias introduced by inter-annual storage changes in the catchments, the mean transpiration was determined based on the 2-year water balance, thus assuming negligible storage change over these years.

The deficits in the months October–April are highly affected by snowfall, as estimates of the effective precipitation are estimated without accounting for snow, leading to soil moisture changes that spread out over an unknown longer period due to the melt process. Therefore, to avoid this influence of snow, only deficits as defined by Eq. (7), in the period of May–September are taken into consideration, which is also the period where deficits are significantly increasing due to relatively low rainfall and high transpiration rates, thus causing soil moisture depletion and drought stress for the vegetation, which in turn, shapes the root zone.

3.2 Model-derived root-zone storage capacity $S_{u,\max}$

The water-balance-derived equilibrium $S_{R,20yr}$ as well as the dynamically changing $S_{R,1yr}$ that reflects regrowth patterns in the years after treatment were compared with estimates of the calibrated parameter $S_{u,\max}$, which represents the mean catchment root-zone storage capacity in lumped conceptual hydrological models. Due to the lack of direct observations of the changes in the root-zone storage capacity, this comparison was used to investigate whether the estimates of the root-zone storage capacity $S_{R,1yr}$, their sensitivity to land-cover change and their effect on hydrological functioning, can provide plausible results. Model-based estimates of root-zone storage capacity may be highly influenced by model formulations and parameterizations. Therefore, four different hydrological models were used to derive the parameter $S_{u,\max}$ in order to obtain a set of different estimates of the catchment-scale root-zone storage capacity. The major features of the model routines for root-zone moisture tested here are briefly summarized below and detailed descriptions including the relevant equations are provided in the Supplement (Sect. S2).

3.2.1 FLEX

The FLEX-based model (Fenicia et al., 2008) was applied in a lumped way to the catchments. The model has nine parameters, eight of which are free calibration parameters, sampled from relatively wide, uniform prior distributions. In contrast, based on the estimation of a Master Recession Curve (e.g. Fenicia et al., 2006), an informed prior distribution between narrow bounds could be used for determining the slow reservoir coefficient K_s.

The model consists of five storage components. First, a snow routine has to be run, which is a simple degree-day module, similar to that used in, for example, HBV (Bergström, 1976). After the snow routine, the precipitation enters the interception reservoir. Here, water evaporates at potential rates or, when exceeding a threshold, directly reaches the soil moisture reservoir. The soil moisture routine is modelled in a similar way to the Xinanjiang model (Zhao, 1992). Briefly, it contains a distribution function that determines the fraction of the catchment where the storage deficit in the root zone is satisfied and that is therefore hydrologically connected to the stream and generating storm runoff. From the soil moisture reservoir, water can further vertically percolate down to recharge the groundwater or leave the reservoir through transpiration. Transpiration is a function of maximum root-zone storage $S_{u,\max}$ and the actual root-zone storage, similar to the functions described by Feddes et al. (1978). Water that cannot be stored in the soil moisture storage is then split into preferential percolation to the groundwater and runoff generating fluxes that enter a fast reservoir, which represents fast-responding system components such as shallow subsurface and overland flow.

3.2.2 HYPE

The HYPE model (Lindström et al., 2010) estimates soil moisture for hydrological response units (HRU), which is the finest calculation unit in this catchment model. In the current set-up, 15 parameters were left free for calibration. Each HRU consists of a unique combination of soil and land-use classes with assigned soil depths. Water input is estimated from precipitation after interception and a snow module at the catchment scale, after which the water enters the three defined soil layers in each HRU. Evaporation and transpiration occurs in the first two layers and fast surface runoff is produced when these layers are fully saturated or when rainfall rates exceeds the maximum infiltration capacities. Water can move between the layers through percolation or laterally via fast flow pathways. The groundwater table is fluctuating between the soil layers with the lowest soil layer normally reflecting the base flow component in the hydrograph. The water balance of each HRU is calculated independently and the runoff is then aggregated in a local stream with routing before entering the main stream.

3.2.3 TUW

The TUW model (Parajka et al., 2007) is a conceptual model with a structure similar to that of HBV (Bergström, 1976) and has 15 free calibration parameters. After a snow module, based on a degree-day approach, water enters a soil moisture routine. From this soil moisture routine, water is partitioned into runoff-generating fluxes and evaporation. Here, transpiration is determined as a function of maximum root-zone storage $S_{u,\max}$ and actual root-zone storage as well. The runoff-generating fluxes percolate into two series of reservoirs. A fast-responding reservoir with overflow outlet represents shallow subsurface and overland flow, while the slower responding reservoir represents the groundwater.

3.2.4 HYMOD

HYMOD (Boyle, 2001) is similar to the applied model structure for FLEX, but only has eight parameters. Besides that, the interception module and percolation from soil moisture to the groundwater are missing. Nevertheless, the model accounts similarly for the partitioning of transpiration and runoff generation in a soil moisture routine. Also for this model, transpiration is a function of maximum storage and actual storage in the root zone. The runoff-generating fluxes are eventually divided over a slow reservoir, representing groundwater, and a fast reservoir, representing the fast processes.

3.2.5 Model calibration

Each model was calibrated using a Monte-Carlo strategy within consecutive 2-year windows in order to obtain a time series of root-zone moisture capacities $S_{u,\max}$. FLEX, TUW

and HYMOD were all run 100 000 times, whereas HYPE was run 10 000 times and 20 000 times for HJ Andrews WS1 and the Hubbard Brook catchments respectively, due to the required runtimes. The Kling–Gupta efficiency for flows (Gupta et al., 2009) and the Kling–Gupta efficiency for the logarithm of the flows were simultaneously used as objective functions in a multi-objective calibration approach to evaluate the model performance for each window. These were selected in order to obtain rather balanced solutions that enable a sufficient representation of peak flows, low flows and the water balance. The unweighted Euclidian distance of the three objective functions served as an informal measure to obtain these balanced solutions (e.g. Hrachowitz et al., 2014; Schoups et al., 2005):

$$L(\theta) = 1 - \sqrt{(1 - E_{\mathrm{KG}})^2 + \left(1 - E_{\mathrm{logKG}}\right)^2}, \tag{8}$$

where $L(\theta)$ is the conditional probability for parameter set θ [–], E_{KG} the Kling–Gupta efficiency [–], E_{logKG} the Kling–Gupta efficiency for the log of the flows [–].

Eventually, a weighing method based on the GLUE-approach of Freer et al. (1996) was applied. To estimate posterior parameter distributions all solutions with Euclidian distances smaller than 1 were maintained as feasible. The posterior distributions were then determined with the Bayes rule (cf. Freer et al., 1996):

$$L_2(\theta) = L(\theta)^n \times L_0(\theta)/C, \tag{9}$$

where $L_0(\theta)$ is the prior parameter distribution [–], $L_2(\theta)$ is the posterior conditional probability [–] , n is a weighing factor (set to 5) [–], and C is a normalizing constant [–]. 5/95th model uncertainty intervals were then constructed based on the posterior conditional probabilities.

3.3 Trend analysis

To test if $S_{\mathrm{R,1yr}}$ significantly changes following de- and subsequent reforestation, which would also indicate shifts in distinct hydrological regimes, a trend analysis, as suggested by Allen et al. (1998), was applied to the $S_{\mathrm{R,1yr}}$ values obtained from the water-balance-based method. As the sampling of interception capacities (Eq. 4) leads to $S_{\mathrm{R,1yr}}$ values for each point in time, which are all equally likely in absence of any further knowledge, the mean of this range was assumed as an approximation of the time-dynamic character of $S_{\mathrm{R,1yr}}$.

Briefly, a linear regression between the full series of the cumulative sums of $S_{\mathrm{R},1yr}$ in the deforested catchment and the unaffected control catchment is established and the residuals and the cumulative residuals are plotted in time. A 95 %-confidence ellipse is then constructed from the residuals:

$$X = \frac{n}{2}\cos(\alpha), \tag{10}$$

$$Y = \frac{n}{\sqrt{n-1}} Z_{p95}\, \sigma_{\mathrm{r}} \sin(\alpha), \tag{11}$$

where X presents the x coordinates of the ellipse (T), Y represents the y coordinates of the ellipse (L), n is the length of the time series (T), α is the angle defining the ellipse (0–2π) between the diagonal of the ellipse and the x axis (–), Z_{p95} is the value belonging to a probability of 95 % of the standard student t-distribution (–) and σ_{r} is the standard deviation of the residuals (assuming a normal distribution) (L).

When the cumulative sums of the residuals plot outside the 95 %-confidence interval defined by the ellipse, the null-hypothesis that the time series are homogeneous is rejected. In that case, the residuals from this linear regression where residual values change from either solely increasing to decreasing or vice versa, can then be used to identify different sub-periods in time.

Thus, in a second step, for each identified sub-period a new regression, with new (cumulative) residuals, can be used to check homogeneity for these sub-periods. In a similar way to before, when the cumulative residuals of these sub-periods now plot within the accompanying newly created 95 %-confidence ellipse, the two series are homogeneous for these sub-periods. In other words, the two time series show consistent behaviour over this particular period.

3.4 Model with time-dynamic formulation of $S_{u,\mathrm{max}}$

In a last step, the FLEX model was reformulated to allow for a time-dynamic representation of the parameter $S_{u,\mathrm{max}}$, reflecting the root-zone storage capacity.

As a reference, the long-term water-balance-derived root-zone storage capacity $S_{\mathrm{R,20yr}}$ was used as a static formulation of $S_{u,\mathrm{max}}$ in the model, and thus kept constant in time. The remaining parameters were calibrated using the calibration strategy outlined above over a period starting with the treatment in the individual catchments until at least 15 years after the end of the treatment. This was done to focus on the period under change (i.e. vegetation removal and recovery), during which the differences between static and dynamic formulations of $S_{u,\mathrm{max}}$ are assumed to be most pronounced.

To test the effect of a dynamic formulation of $S_{u,\mathrm{max}}$ as a function of forest regrowth, the calibration was run with a temporally evolving series of root-zone storage capacity. The time-dynamic series of $S_{u,\mathrm{max}}$ were obtained from a relatively simple growth function, the Weibull function (Weibull, 1951):

$$S_{u,\mathrm{max}}(t) = S_{\mathrm{R,20yr}} \left(1 - e^{-at^b}\right), \tag{12}$$

where $S_{u,\mathrm{max}}(t)$ is the root-zone storage capacity t time steps after reforestation (L), $S_{\mathrm{R,20yr}}$ is the equilibrium value (L),

and a (T^{-1}) and b (–) are shape parameters. In the absence of more information, this equation was selected as the first, simple way of incorporating the time-dynamic character of the root-zone storage capacity in a conceptual hydrological model. In this way, root growth is exclusively determined dependent on time, whereas the shape parameters a and b merely implicitly reflect the influence of other factors, such as climatic forcing, in a lumped way. These parameters were estimated based on qualitative judgement so that $S_{u,\max}(t)$ coincides well with the suite of S_{R1yr} values after logging. In other words, the values were chosen by trial and error in such a way that the time-dynamic formulation of $S_{u,\max}(t)$ shows a visually good correspondence with the S_{R1yr} values. This approach was followed to filter out the short-term fluctuations in the S_{R1yr} values, which is not warranted by this equation. Note that this rather simple approach is merely meant as a proof of concept for a dynamic formulation of $S_{u,\max}$.

In addition, the remaining parameter directly related to vegetation, the interception capacity ($I_{\max}$), was also assigned a time-dynamic formulation. Here, the same growth function was applied (Eq. 12), but the shape of the growth function was assumed fixed (i.e. growth parameters a and b were fixed to values of 0.001 (day^{-1}) and 1 (–)) loosely based on the posterior ranges of the window calibrations, with qualitative judgement as well. This growth function was used to ensure the degrees of freedom for both the time-variant and the time-invariant models, leaving the equilibrium value of the interception capacity as the only free calibration parameter for this process. Note that the empirically parameterized growth functions can be readily extended and/or replaced by more mechanistic, process-based descriptions of vegetation growth if warranted by the available data, and they were here merely used to test the effect of considering changes in vegetation on the skill of models to reproduce hydrological response dynamics.

To assess the performance of the dynamic model compared to the time-invariant formulation, beyond the calibration objective functions, model skill in reproducing 28 hydrological signatures was evaluated (Sivapalan et al., 2003). Even though the signatures are not always fully independent of each other, this larger set of measures allows a more complete evaluation of the model skill as, ideally, the model should be able to simultaneously reproduce all signatures. An overview of the signatures is given in Table 3. The results of the comparison were quantified on the basis of the probability of improvement for each signature (Nijzink et al., 2016):

$$P_{I,S} = P\left(S_{\mathrm{dyn}} > S_{\mathrm{stat}}\right) = \sum_{i=1}^{n} P\left(S_{\mathrm{dyn}} > S_{\mathrm{stat}} \mid S_{\mathrm{dyn}} = r_i\right) P\left(S_{\mathrm{dyn}} = r_i\right), \quad (13)$$

where S_{dyn} and S_{stat} are the distributions of the signature performance metrics of the dynamic and static model, respectively, for the set of all feasible solutions retained from calibration, r_i is a single realization from the distribution of S_{dyn} and n is the total number of realizations of the S_{dyn} distribution. For $P_{I,S} > 0.5$ it is then more likely that the dynamic model outperforms the static model with respect to the signature under consideration, and vice versa for $P_{I,S} < 0.5$. The signature performance metrics that were used are the relative error (for single-valued signatures) and the Nash–Sutcliffe efficiency (Nash and Sutcliffe, 1970), for signatures that represent a time series.

In addition, as a more quantitative measure, the ranked probability score, giving information on the magnitude of model improvement or deterioration, was calculated (Wilks, 2005):

$$S_{\mathrm{RP}} = \frac{1}{M-1} \sum_{m=1}^{M} \left[\left(\sum_{k=1}^{m} p_k \right) - \left(\sum_{k=1}^{m} o_k \right) \right]^2, \quad (14)$$

where M is the number of feasible solutions, p_k the probability of a certain signature performance to occur and o_k the probability of the observation to occur (either 1 or 0, as there is only a single observation). Briefly, the S_{RP} represents the area enclosed between the cumulative probability distribution obtained by model results and the cumulative probability distribution of the observations. Thus, when modelled and observed cumulative probabilities are identical, the enclosed area goes to zero. Therefore, the difference between the S_{RP} for the feasible set of solutions for the time-variant and time-invariant model formulation was used in the comparison, identifying which model is quantitatively closer to the observation.

4 Results

4.1 Deforestation and changes in hydrological response dynamics

We found that the three deforested catchments in the two research forests show on balance similar response dynamics after the logging of the catchments (Fig. 2). This supports the findings from previous studies of these catchments (Andréassian, 2004; Bosch and Hewlett, 1982; Hornbeck et al., 1997; Rothacher et al., 1967). More specifically, it was found that the observed annual runoff coefficients for HJ Andrews WS1 and Hubbard Brook WS2 (Fig. 2a, b) change after logging of the catchments, also in comparison with the adjacent, undisturbed reference watersheds. Right after deforestation, runoff coefficients increase, followed by a gradual decrease.

The annual autocorrelation coefficients with a 1-day lag time are generally lower after logging than in the years before the change, which can be seen in particular from Fig. 2e and f as here a long pre-treatment time series record is available. Nevertheless, the climatic influence cannot be ignored here, as the reference watershed shows a similar pattern. Only for Hubbard Brook WS5 (Fig. 2f) does the autocorrelation show reduced values in the first years after logging. Thus, the flows

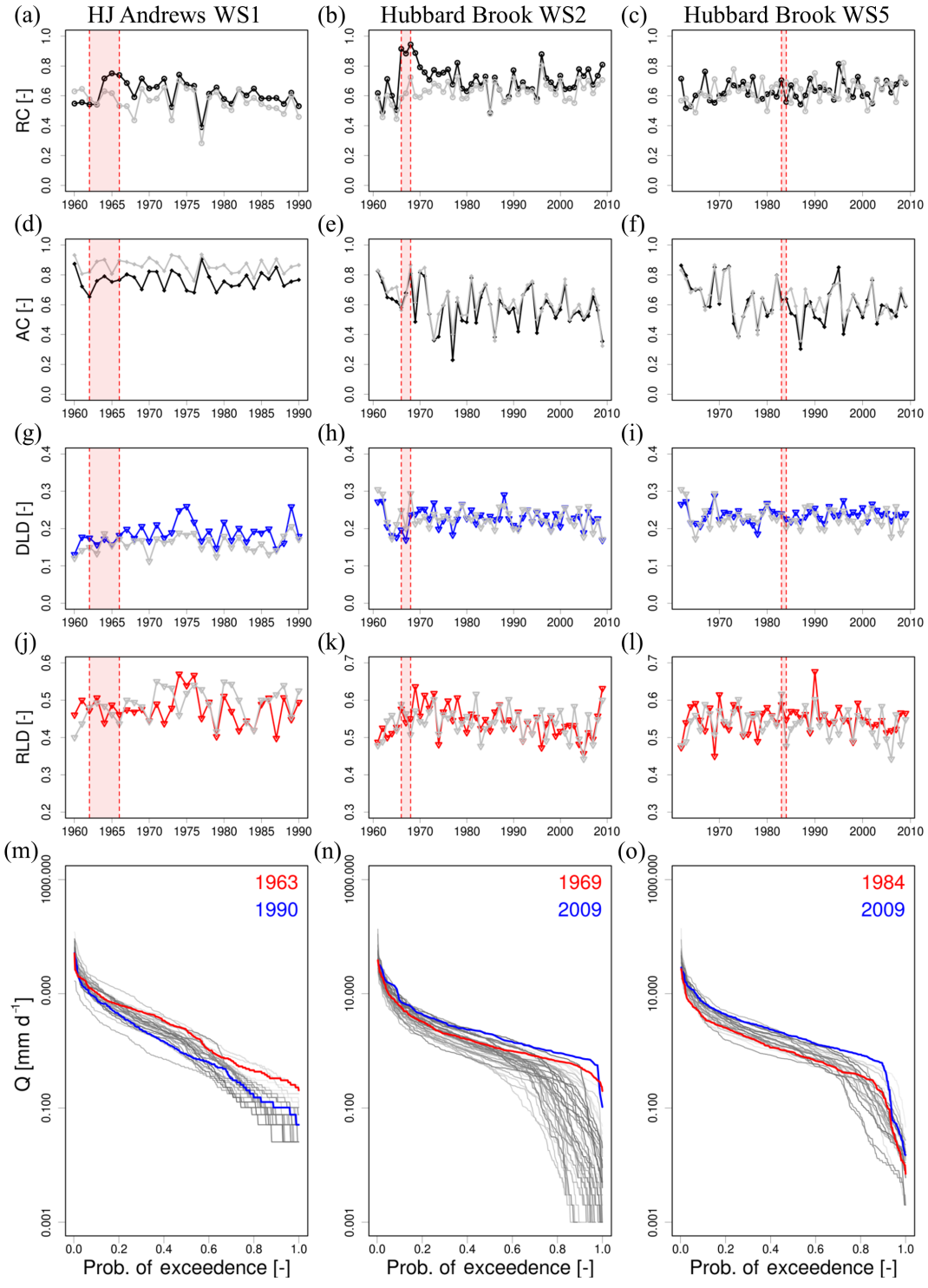

Figure 2. Evolution of signatures in time of (**a–c**) the runoff coefficient, (**d–f**) the 1-day autocorrelation, (**g–i**) the declining limb density, (**j–l**) the rising limb density with the reference watersheds in grey and periods of deforestation in red shading. The flow duration curves for HJ Andrews WS1, Hubbard Brook WS2 and Hubbard Brook WS5 are shown in **(m)–(o)**, where years between the first and last year are coloured from light gray to dark grey as they progress in time.

Table 3. Overview of the hydrological signatures.

Signature	Description	Reference
S_{QMA}	Mean annual runoff	
S_{AC}	One day autocorrelation coefficient	Montanari and Toth (2007)
$S_{\mathrm{AC,summer}}$	One day autocorrelation the summer period	Euser et al. (2013)
$S_{\mathrm{AC,winter}}$	One day autocorrelation the winter period	Euser et al. (2013)
S_{RLD}	Rising limb density	Shamir et al. (2005)
S_{DLD}	Declining limb density	Shamir et al. (2005)
S_{Q_5}	Flow exceeded in 5 % of the time	Jothityangkoon et al. (2001)
$S_{Q_{50}}$	Flow exceeded in 50 % of the time	Jothityangkoon et al. (2001)
$S_{Q_{95}}$	Flow exceeded in 95 % of the time	Jothityangkoon et al. (2001)
$S_{Q_5,\mathrm{summer}}$	Flow exceeded in 5 % of the summer time	Yilmaz et al. (2008)
$S_{Q_{50},\mathrm{summer}}$	Flow exceeded in 50 % of the summer time	Yilmaz et al. (2008)
$S_{Q_{95},\mathrm{summer}}$	Flow exceeded in 95 % of the summer time	Yilmaz et al. (2008)
$S_{Q_5,\mathrm{winter}}$	Flow exceeded in 5 % of the winter time	Yilmaz et al. (2008)
$S_{Q_{50},\mathrm{winter}}$	Flow exceeded in 50 % of the winter time	Yilmaz et al. (2008)
$S_{Q_{95},\mathrm{winter}}$	Flow exceeded in 95 % of the winter time	Yilmaz et al. (2008)
S_{Peaks}	Peak distribution	Euser et al. (2013)
$S_{\mathrm{Peaks,summer}}$	Peak distribution summer period	Euser et al. (2013)
$S_{\mathrm{Peaks,winter}}$	Peak distribution winter period	Euser et al. (2013)
$S_{Q_{\mathrm{peak},10}}$	Flow exceeded in 10 % of the peaks	
$S_{Q_{\mathrm{peak},50}}$	Flow exceeded in 50 % of the peaks	
$S_{Q_{\mathrm{summer,peak},10}}$	Flow exceeded in 10 % of the summer peaks	
$S_{Q_{\mathrm{summer,peak},50}}$	Flow exceeded in 10 % of the summer peaks	
$S_{Q_{\mathrm{winter,peak},10}}$	Flow exceeded in 10 % of the winter peaks	
$S_{Q_{\mathrm{winter,peak},50}}$	Flow exceeded in 50 % of the winter peaks	
S_{SFDC}	Slope flow duration curve	Yadav et al. (2007)
S_{LFR}	Low flow ratio (Q_{90} / Q_{50})	
S_{FDC}	Flow duration curve	Westerberg et al. (2011)
$S_{\mathrm{AC,serie}}$	Autocorrelation series (200 days lag time)	Montanari and Toth (2007)

at any time $t+1$ are less dependent on the flows at t, which points towards less memory and thus less storage in the system (i.e. reduced S_{R}), leading to increased peak flows, similar to the reports of, for example, Patric and Reinhart (1971) for one of the Fernow experiments.

The declining limb density for HJ Andrews WS1 (Fig. 2g) shows increased values right after deforestation, whereas a longer time after deforestation, the values seem to plot closer to the values obtained from the reference watershed. This indicates that for the same number of peaks, less time was needed for the recession in the hydrograph in the early years after logging. In contrast, the rising limb density shows increased values during and right after deforestation for Hubbard Brook WS2 and WS5 (Fig. 2k–l), compared to the reference watershed. Here, less time was needed for the rising part of the hydrograph in the more early years after logging. Thus, the recession seems to be affected in HJ Andrews WS1, whereas the Hubbard Brook watersheds exhibit a quicker rise of the hydrograph.

Eventually, the flow duration curves, as shown in Fig. 2m–o, indicate a higher variability of flows, as the years following deforestation plot with an increased steepness of the flow duration curve, i.e. a higher flashiness. This increased flashiness of the catchments after deforestation can also be noted from the hydrographs shown in Fig. 3. The peaks in the hydrographs are generally higher, and the flows return faster to the baseflow values in the years right after deforestation than some years later after some forest regrowth, all with similar values for the yearly sums of precipitation and potential evaporation.

4.2 Temporal evolution of S_{R} and $S_{u,\mathrm{max}}$

The observed changes in the hydrological response of the study catchments (as discussed above) were also clearly reflected in the temporal evolution of the root-zone storage capacities as described by the catchment models (Fig. 4). The models all exhibited Kling–Gupta efficiencies ranging between 0.5 and 0.8 and Kling–Gupta efficiencies of the log of the flows between 0.2 and 0.8 (see the Supplement Figs. S5–S7, with all posterior parameter distributions in Figs. S10–S27, and the number of feasible solutions in Tables S5–S7 in the Supplement). Comparing the water-balance- and model-derived estimates of root-zone storage capacity S_{R} and $S_{u,\mathrm{max}}$, respectively, then showed that they exhibit very similar patterns in the study catchments. Especially for HJ

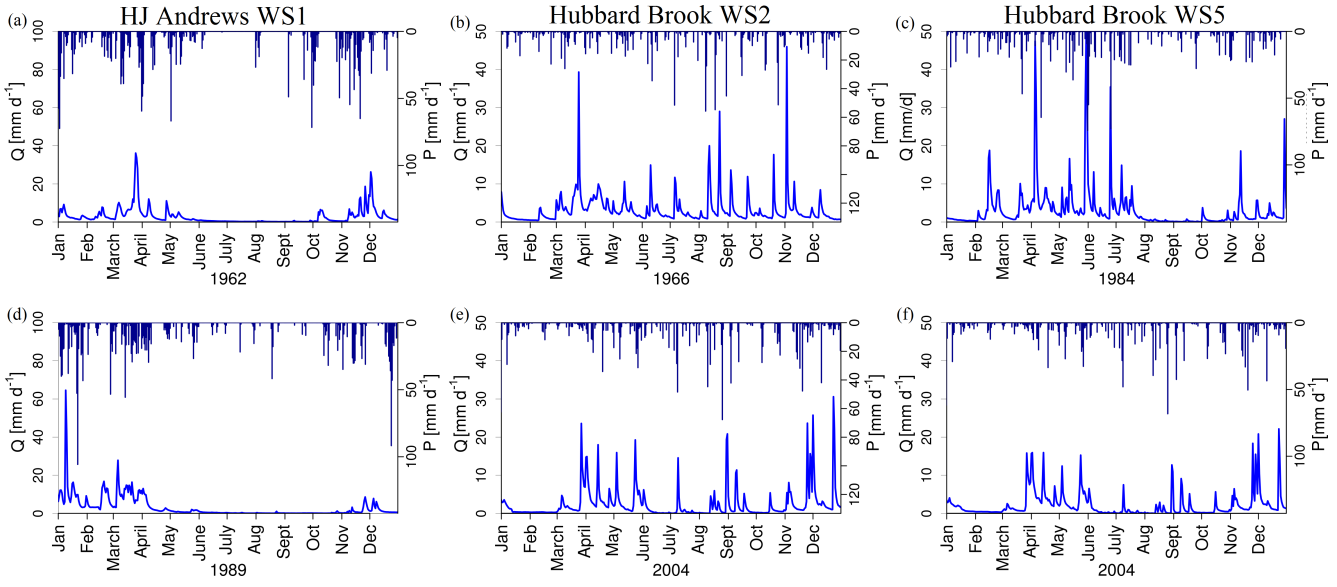

Figure 3. Hydrographs for HJ Andrews WS1 in **(a)** 1962 (annual precipitation $P_A = 2018$, $E_{p,A} = 951\,\mathrm{mm\,yr^{-1}}$) and **(b)** 1989 ($P_A = 1752$, $E_{p,A} = 846\,\mathrm{mm\,yr^{-1}}$), Hubbard Brook WS2 in **(c)** 1966 ($P_A = 1222$, $E_{p,A} = 788\,\mathrm{mm\,yr^{-1}}$ and **(d)** 2004 ($P_A = 1296$, annual $E_{p,A} = 761\,\mathrm{mm\,yr^{-1}}$ and Hubbard Brook WS5 in **(e)** 1984 ($P_A = 1480$, annual $E_{p,A} = 721\,\mathrm{mm\,yr^{-1}}$) and **(f)** 2004 ($P_A = 1311$, $E_{p,A} = 731\,\mathrm{mm\,yr^{-1}}$).

Andrews WS1 and Hubbard Brook WS2, root-zone storage capacities sharply decreased after deforestation and gradually recovered during regrowth towards a dynamic equilibrium of climate and vegetation, whereas the undisturbed reference catchments of HJ Andrews WS2 and Hubbard Brook WS3 showed a rather constant signal over the full period (see Fig. S8).

The HJ Andrews WS1 shows the clearest signal when looking at the water-balance-derived S_R, as can be seen by the green shaded area in Fig. 4a. Before deforestation, the root-zone storage capacity $S_{R,1yr}$ was found to be around 400 mm. During deforestation, the $S_{R,1yr}$ required to provide the remaining vegetation with sufficient and continuous access to water decreased from around 400 to 200 mm. For the first 4–6 years after deforestation the $S_{R,1yr}$ increased again, reflecting the increased water demand of vegetation with the regrowth of the forest. In addition, it was observed that in the period 1971–1978 $S_{R,1yr}$ slowly decreased again in HJ Andrews.

The four models show a similar pronounced decrease of the calibrated, feasible set of $S_{u,max}$ during deforestation and a subsequent gradual increase over the first years after deforestation. The model concepts, and thus our assumptions about nature, can therefore only account for the changes in hydrological response dynamics of a catchment, when calibrated in a window calibration approach with different parameterizations for each time frame. The absolute values of $S_{u,max}$ obtained from the most parsimonious HYMOD and FLEX models (both with 8 free calibration parameters) show a somewhat higher similarity to $S_{R,1yr}$ and its temporal evolution than the values from the other two models. In spite of similar general patterns in $S_{u,max}$, the higher number of parameters in TUW (i.e. 15) result, due to compensation effects between individual parameters, in wider uncertainty bounds which are less sensitive to change. It was also observed that in particular TUW overestimates $S_{u,max}$ compared to $S_{R,1yr}$, which can be attributed to the absence of an interception reservoir, leading to a root zone that has to satisfy not only transpiration but all evaporative fluxes.

Hubbard Brook WS2 exhibits a similarly clear decrease in root-zone storage capacity as a response to deforestation, as shown in Fig. 4b. The water-balance-based $S_{R,1yr}$ estimates approach values of zero during and right after deforestation. In these years the catchment was treated with herbicides, removing effectively any vegetation, thereby minimizing transpiration. In this catchment a more gradual regrowth pattern occurred, which continued after logging started in 1966 until around 1983.

Generally, the models applied in Hubbard Brook WS2 show similar behaviour to those in the HJ Andrews catchment. The calibrated $S_{u,max}$ clearly follows the temporal pattern of $S_{R,1yr}$, reflecting the pronounced effects of de- and reforestation. It can, however, also be observed that the absolute values of $S_{u,max}$ exceed the $S_{R,1yr}$ estimates. While FLEX on balance exhibits the closest resemblance between the two values, the TUW model in particular exhibits wide uncertainty bounds with elevated $S_{u,max}$ values. Besides the role of interception evaporation, which is only explicitly accounted for in FLEX, the results are also linked to the fact that the humid climatic conditions with little seasonality re-

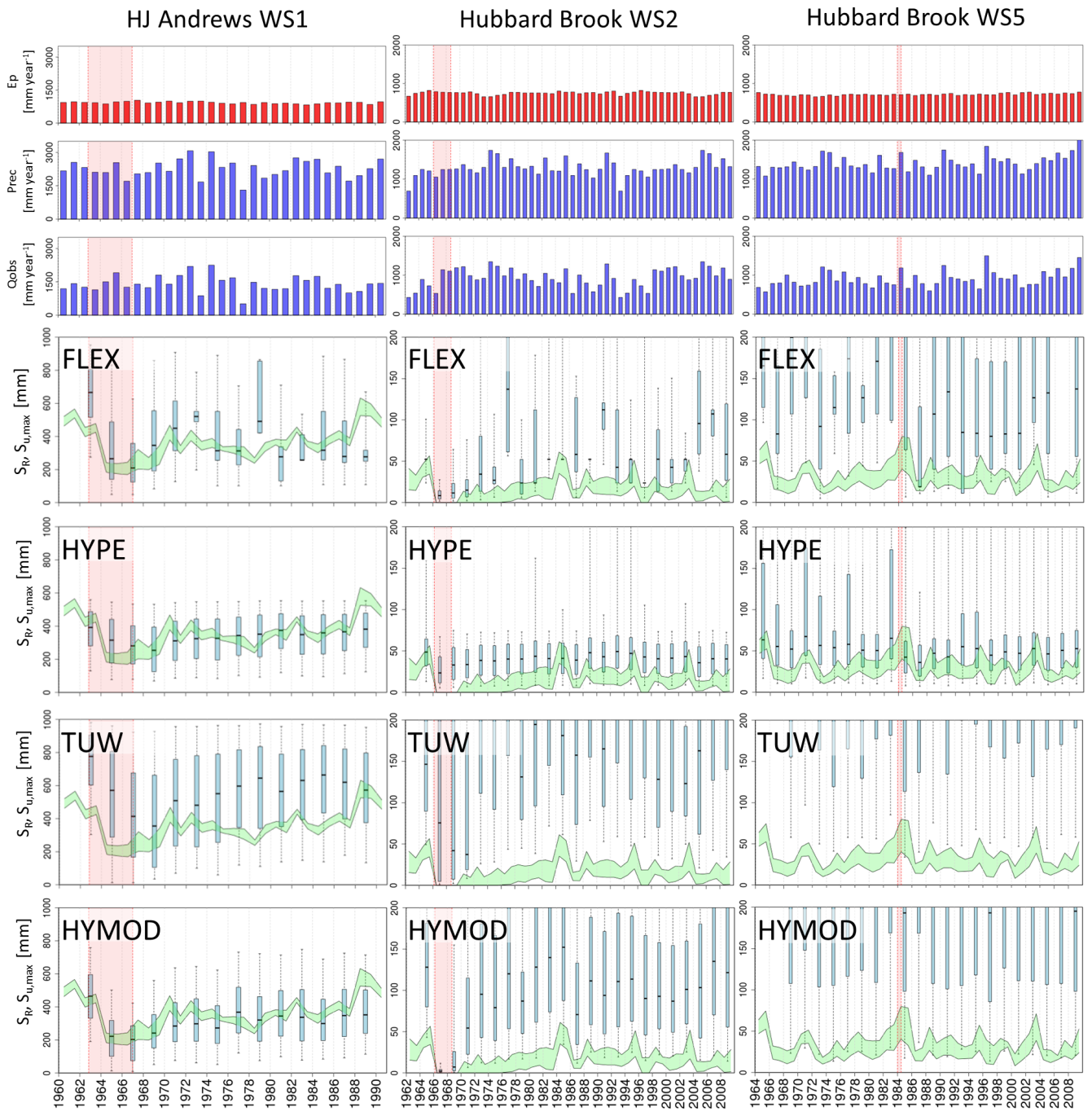

Figure 4. Evolution of root-zone storage capacity $S_{R,1yr}$ from water balance-based estimation (green shaded area, a range of solutions due to the sampling of the unknown interception capacity) compared with $S_{u,\max,2yr}$ estimates obtained from the calibration of four models (FLEX, HYPE, TUW, HYMOD; blue box plots) for HJ Andrews WS1, Hubbard Brook WS2 and Hubbard Brook WS5. Red shaded areas are periods of deforestation.

duces the importance of the model parameter $S_{u,\max}$, and makes it thereby more difficult to identify by calibration. The parameter is most important for lengthy dry periods when vegetation needs enough storage to ensure continuous access to water.

The temporal variation in S_R in Hubbard Brook WS5 does not show such a distinct signal as in the other two study catchments (Fig. 4c). Moreover, it can be noted that in the summers of 1984 and 1985 the values of $S_{R,1yr}$ are relatively high. Nevertheless, the model-based values of $S_{u,\max}$ show again similar dynamics to the water-balance-based $S_{R,1yr}$ val-

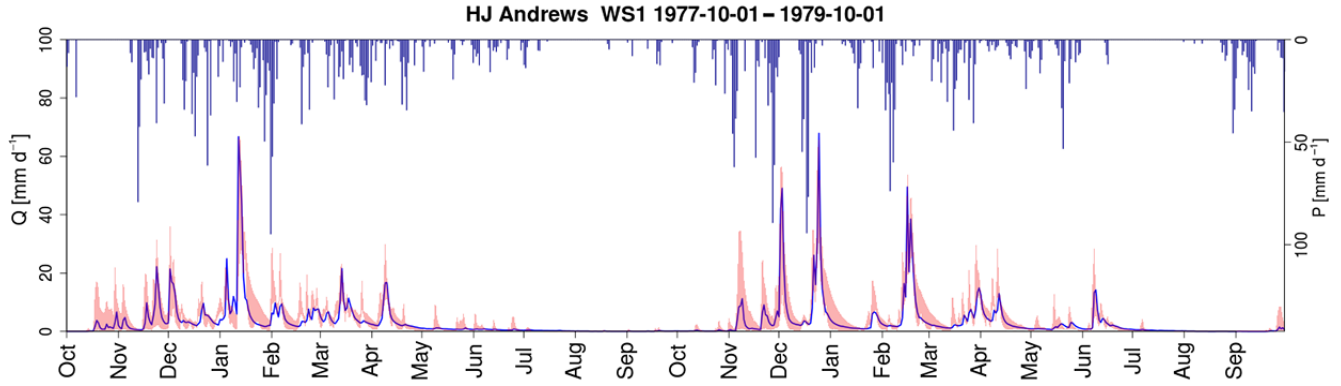

Figure 5. Observed and modelled hydrograph for HJ Andrews WS1 for the years of 1978 and 1979, with the red coloured area indicating the 5/95 % uncertainty intervals of the modelled discharge. Blue bars show daily precipitation.

ues. TUW and HYMOD show again higher model-based values, but FLEX is also now overestimating the root-zone storage capacity.

4.3 Process understanding – trend analysis and change in hydrological regimes

The trend analysis for water-balance-derived values of $S_{R,1yr}$ suggests that for all three study catchments significantly different hydrological regimes in time can be identified before and after deforestation, linked to changes in $S_{R,1yr}$ (Fig. 7). For all three catchments, the cumulative residuals plot outside the 95 %-confidence ellipse, indicating that the time series obtained in the control catchments and the deforested catchments are not homogeneous (Fig. 7g–i).

Rather obvious break points can be identified in the residuals plots for the catchments HJ Andrews WS1 and Hubbard Brook WS2 (Fig. 7d–e). Splitting up the $S_{R,1yr}$ time series according to these break points into the periods before deforestation, deforestation and recovery resulted in three individually homogenous time series that are significantly different from each other, indicating switches in the hydrological regimes. The results shown in Fig. 4 indicate that these catchments developed a rather stable root-zone storage capacity sometime after the start of deforestation (for HJ Andrews WS1 after 1964, for Hubbard Brook WS2 after 1967). Hence, recovery and deforestation balanced each other, leading to a temporary equilibrium. The recovery signal then becomes more dominant in the years after deforestation. The third homogenous period suggests that the root-zone storage capacity reached a dynamic equilibrium without any further systematic changes. This can be interpreted in the way that in the HJ Andrews WS1, hydrological recovery after deforestation due to the recovery of the root-zone storage capacity took about 6–9 years (Fig. 7p), while Hubbard Brook WS2 required 10–13 years for hydrological recovery (Fig. 7q). This strongly supports the results of Hornbeck et al. (2014), who reported changes in water yield for WS2 for up to 12 years after deforestation.

The identification of different periods is less obvious for Hubbard Brook WS5, but the two time series of control catchment and treated catchment are significantly different (see the cumulative residuals in Fig. 7i). Nevertheless, the most obvious break point in residuals can be found in 1989 (Fig. 7f). In addition, it can be noted that turning points also exist in 1983 and 1985. These years can be used to split the time series into four groups (leading to the periods of 1964–1982, 1983–1985, 1986–1989 and 1990–2009 for further analysis). The cumulative residuals from the new regressions, based on the grouping, plot within the confidence bounds again, and show a period with deforestation (1983–1985) and recovery (1986–1989). Mou et al. (1993) reported similar findings with the highest biomass accumulation in 1986 and 1988, and slower vegetation growth in the early years. Therefore, full recovery took 5–6 years in Hubbard Brook WS5.

4.4 Time-variant model formulation

The adjusted model routine for FLEX, which uses a dynamic time series of $S_{u,max}$, generated with the Weibull growth function (Eq. 12), resulted in a rather small impact on the overall model performance in terms of the calibration objective function values (Fig. 8b, d, f) compared to the time-invariant formulation of the model. The strongest improvements for calibration were observed for the dynamic formulation of FLEX for HJ Andrews WS1 and Hubbard Brook WS2 (Fig. 8b and d), which reflects the rather clear signal from deforestation in these catchments.

Evaluating a set of hydrological signatures suggests that the dynamic formulation of $S_{u,max}$ allows the model to have a higher probability of better reproducing most of the signatures tested here (51 % of all signatures in the three catchments) as shown in Fig. 9a. A similar pattern is obtained for the more quantitative S_{RP} (Fig. 9b), where in 52 % of

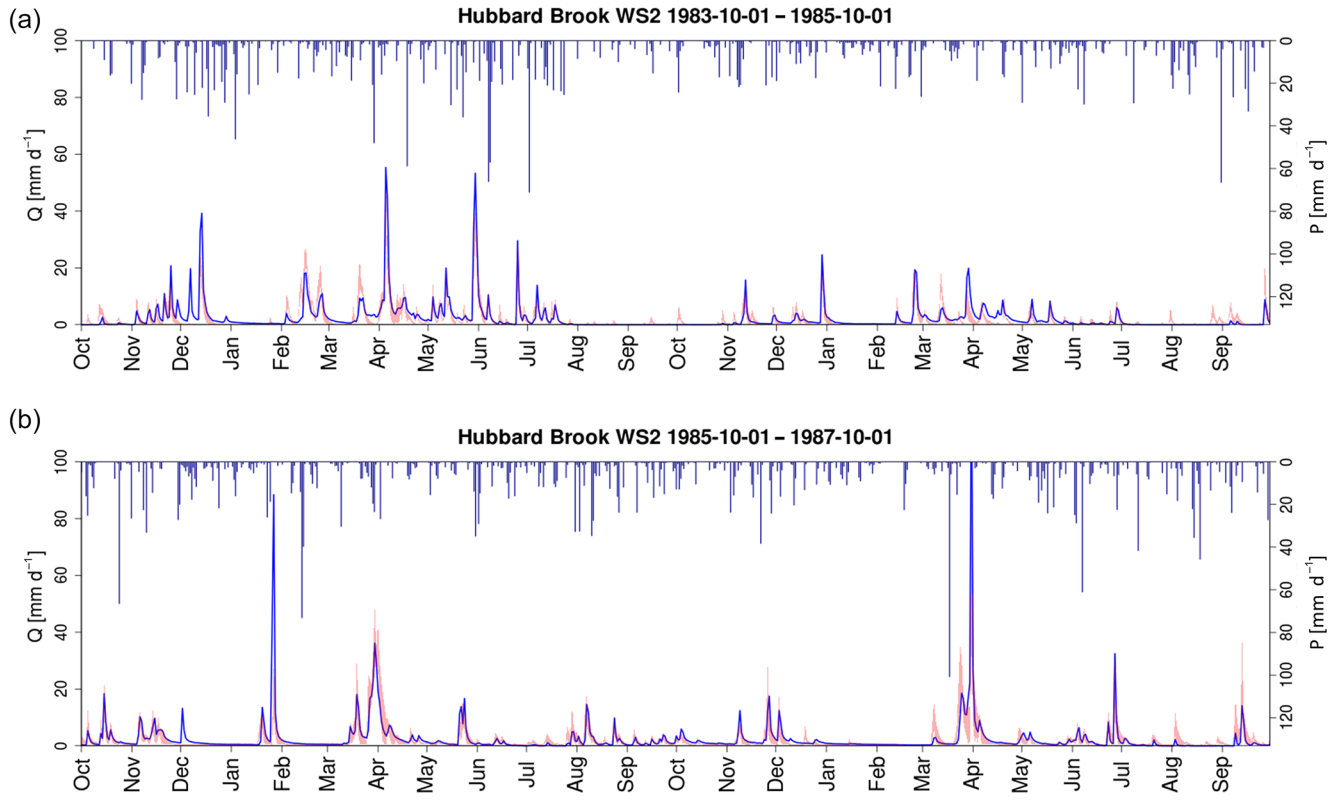

Figure 6. Observed and modelled hydrograph for Hubbard Brook WS2 for **(a)** the years of 1984 and 1985 and **(b)** the years of 1986 and 1987, with the red coloured area indicating the 5/95 % uncertainty intervals of the modelled discharge. Blue bars show daily precipitation.

the cases improvements are observed. Most signatures for HJ Andrews WS1 show a high probability of improvement, with a maximum $P_{I,S} = 0.69$ (for $S_{Q95,winter}$) and an average $P_{I,S} = 0.55$. Considering the large difference between the deforested situation and the new equilibrium situation of about 200 mm, this supports the hypothesis that here a time-variant formulation of $S_{u,\max}$ does provide means for an improved process representation and, thus, hydrological signatures. Here, improvements are observed especially in the high flows in summer ($S_{Q5,\text{summer}}$, $S_{Q50,\text{summer}}$) and peak flows (e.g. S_{Peaks}, $S_{\text{Peaks,summer}}$, $S_{\text{Peaks,winter}}$), which illustrates that the root-zone storage affects mostly the fast-responding components of the system.

At Hubbard Brook WS2 a more variable pattern is shown in the ability of the model to reproduce the hydrological signatures. It is interesting to note that the low flows (S_{Q95}, $S_{Q95,\text{summer}}$, $S_{Q50,\text{summer}}$) improve, opposed to the expectation raised by the argumentation for HJ Andrews WS1 that peak flows and high flows should improve. In this case, the peaks are too high for the time-dynamic model.

The probabilities of improvement for the signatures in Hubbard Brook WS5 show an even less clear signal: the model cannot clearly identify a preference for either a dynamic or static formulation of $S_{u,\max}$ (relatively white colours in Fig. 9). This absence of a clear preference can be related to the observed patterns in water-balance-derived S_R (Fig. 4c), which also does not show a very clear signal after deforestation, indicating that the root-zone storage capacity is of less importance in this humid region characterized by limited seasonality.

5 Discussion

5.1 Deforestation and changes in hydrological response dynamics

The changes found in the runoff behaviour of the deforested catchments point towards shifts in the yearly sums of transpiration, which can, except for climatic variation, be linked to the regrowth of vegetation that takes place at a similar pace to the changes in hydrological dynamics. This coincidence of regrowth dynamics and evolution of runoff coefficients was not only noticed by Hornbeck et al. (2014) for the Hubbard Brook, but was also previously acknowledged for example by Swift and Swank (1981) in the Coweeta experiment or Kuczera (1987) for eucalypt regrowth after forest fires.

Therefore, the key role of vegetation in this partitioning between runoff and transpiration (Donohue et al., 2012), or more specifically root zones (Gentine et al., 2012), necessarily leads to a change in runoff coefficients when vegeta-

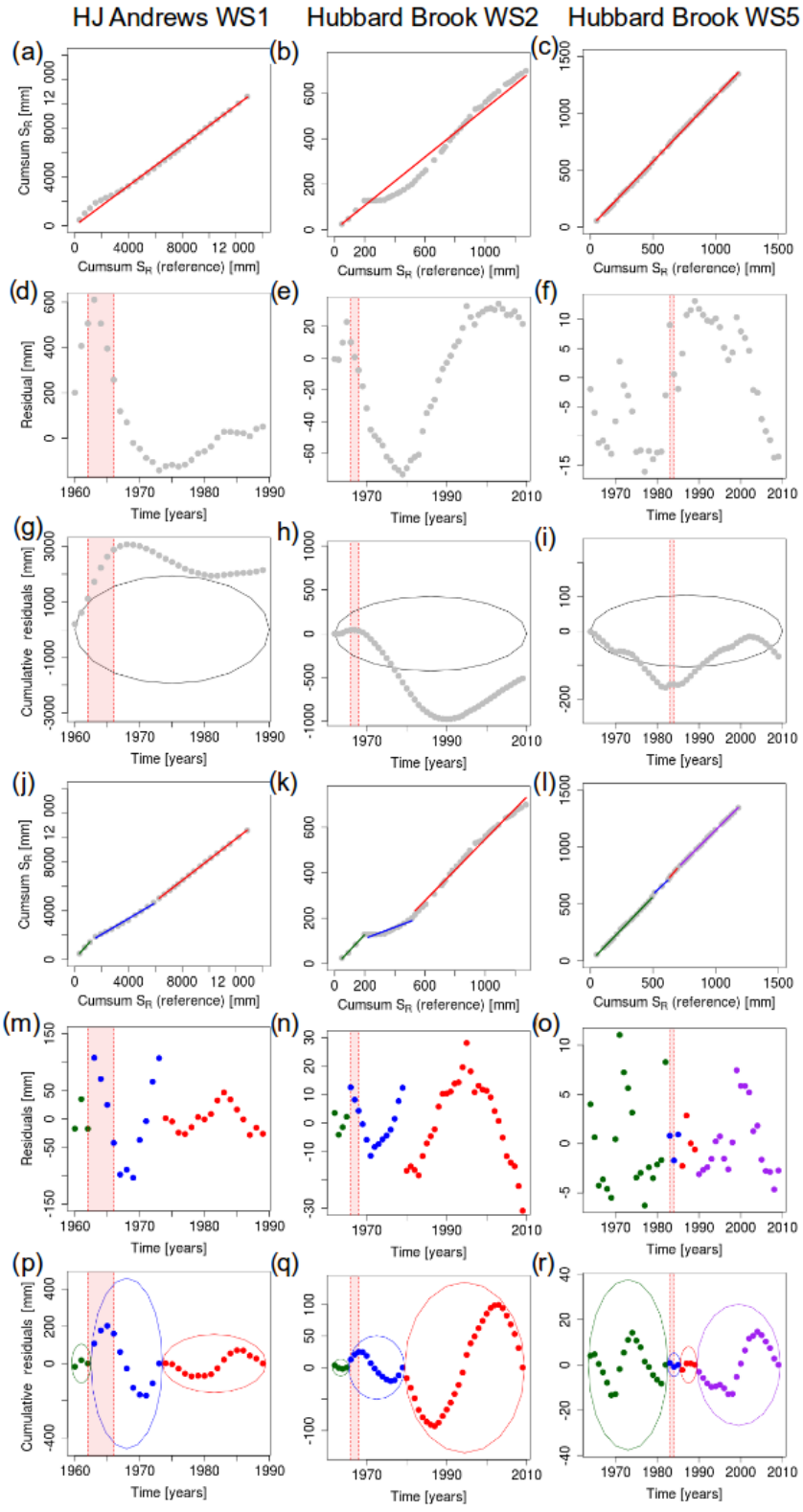

Figure 7. Trend analysis for $S_{R,1yr}$ in HJ Andrews WS1, Hubbard Brook WS2 and WS5 based on comparison with the control watersheds with (**a**–**c**) cumulative root-zone storages ($S_{R,1yr}$) with regression, (**d**–**f**) residuals of the regression of cumulative root-zone storages, (**g**–**i**) significance test; the cumulative residuals do not plot within the 95 %-confidence ellipse, rejecting the null-hypothesis that the two time series are homogeneous, (**j**–**l**) piecewise linear regression based on break points in residuals plot, (**m**–**o**) residuals of piecewise linear regression, (**p**–**r**) significance test based on piecewise linear regression with homogeneous time series of $S_{R,1yr}$. The different colours (green, blue, red, violet) indicate individual homogeneous time periods.

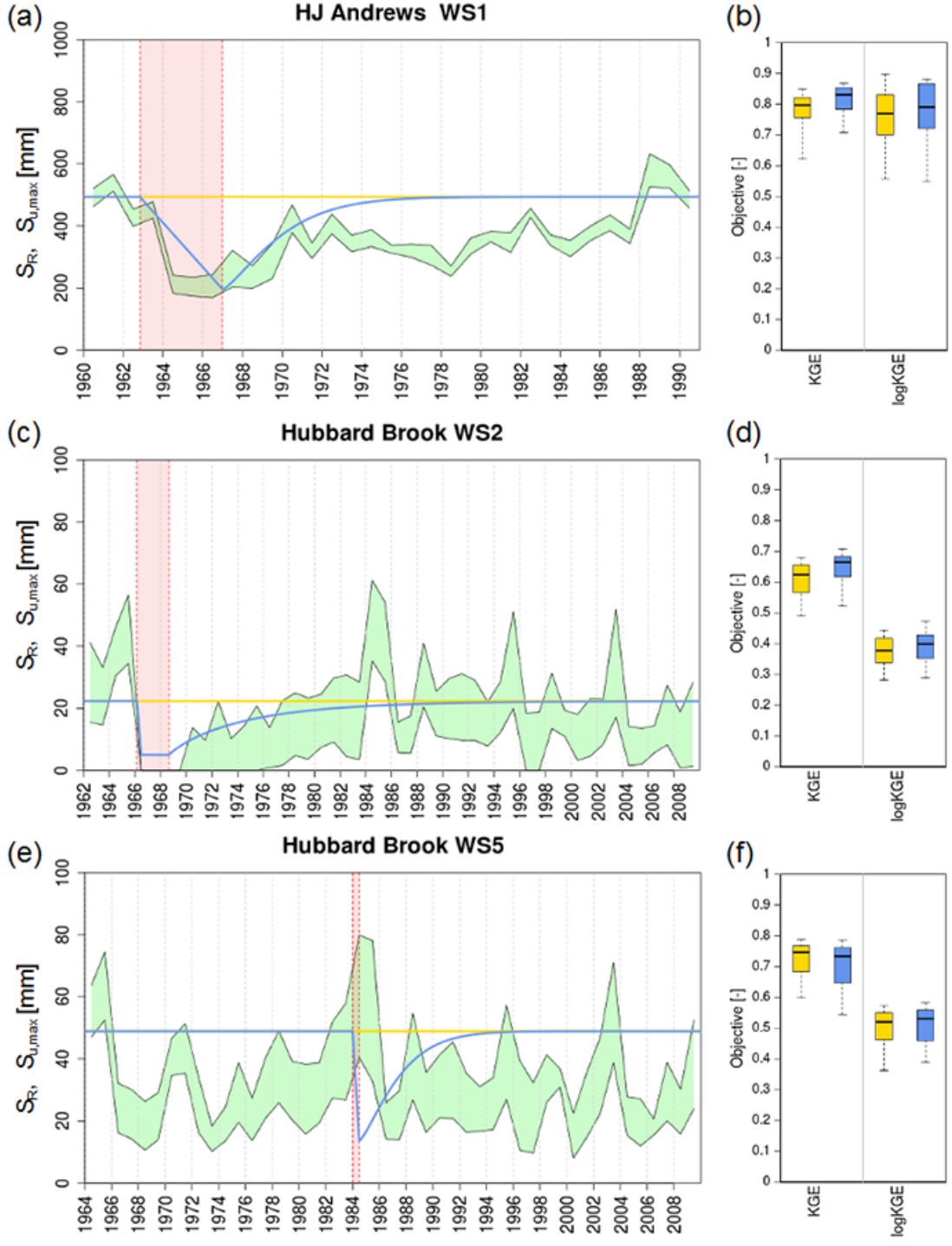

Figure 8. The time invariant $S_{u,\max}$ formulation represented by $S_{\mathrm{R},20\mathrm{yr}}$ (yellow) and time dynamic $S_{u,\max}$ fitted Weibull growth function (blue) with a linear reduction during deforestation (red shaded area) and mean 20-year return period root-zone storage capacity $S_{\mathrm{R},\,20\mathrm{yr}}$ as equilibrium value for **(a)** HJ Andrews WS1 with $a = 0.0001$ days^{-1}, $b = 1.3$ and $S_{\mathrm{R},20\mathrm{yr}} = 494$ mm with **(b)** the objective function values, **(c)** Hubbard Brook WS2 with $a = 0.001$ days^{-1}, $b = 0.9$ and $S_{\mathrm{R},20\mathrm{yr}} = 22$ mm with **(d)** the objective function values, and **(e)** Hubbard Brook WS5 with $a = 0.001$ days^{-1}, $b = 0.9$ and $S_{\mathrm{R},20\mathrm{yr}} = 49$ mm and with **(f)** the objective function values. The green shaded area represents the maximum and minimum boundaries of $S_{\mathrm{R},1\mathrm{yr}}$ from the water balance-based estimation, caused by the sampling of interception capacities.

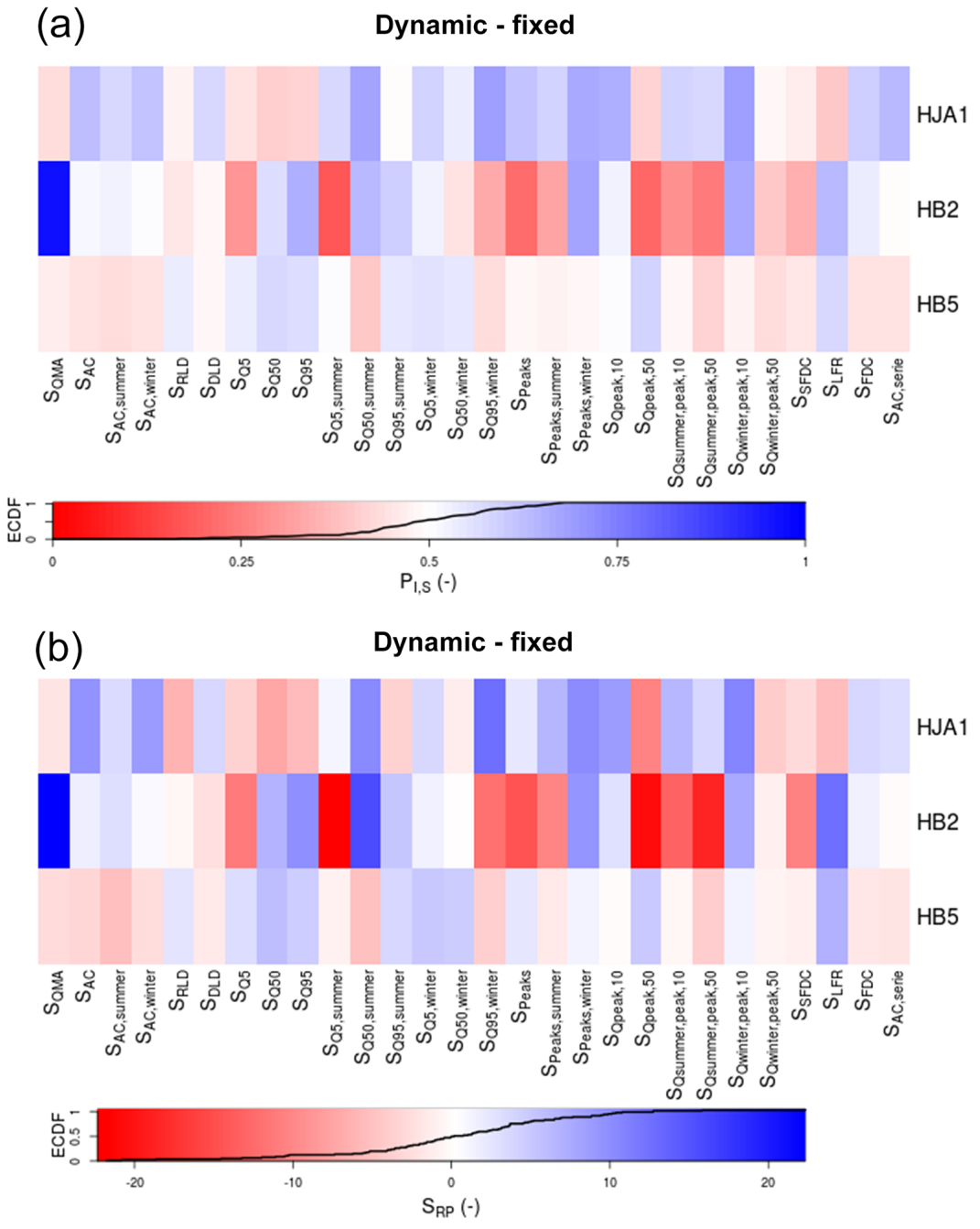

Figure 9. Signature comparison between a time-dynamic and time-invariant formulation of root-zone storage capacity in the FLEX model with **(a)** probabilities of improvement and **(b)** Ranked Probability Score for 28 hydrological signatures for HJ Andrews WS1 (HJA1), Hubbard Brook WS2 (HB2) and Hubbard Brook WS5 (HB5). High values are shown in blue, whereas a low values are shown in red.

tion is removed. Similarly, Gao et al. (2014) found a strong correlation between root-zone storage capacities and runoff coefficients in more than 300 US catchments, which lends further support to the hypothesis that root-zone storage capacities may have decreased in deforested catchments right after removal of the vegetation.

5.2 Temporal evolution of S_R and $S_{u,max}$

The differences between the Hubbard Brook catchments and HJ Andrews catchments can be related to climatic conditions. In spite of the high annual precipitation volumes, high $S_{R,1yr}$ values are plausible for HJ Andrews WS1 given the marked seasonality of the precipitation in the Mediterranean climate

(Köppen–Geiger class Csb) and the approximately 6-month phase shift between precipitation and potential evaporation peaks in the study catchment, which dictates that the storage capacities need to be large enough to store precipitation, which falls mostly during winter, throughout the extended dry periods with higher energy supply throughout the rest of the year (Gao et al., 2014). At the same time, low $S_{R,1yr}$ values in Hubbard Brook WS2 can be related to the relatively humid climate, and the absence of pronounced rainfall seasonality strongly reduces storage requirements.

It can also be argued that there is a strong influence of the inter-annual climatic variability on the estimated root-zone storage capacities. For example, the marked increase in $S_{R,1yr}$ in Hubbard Brook WS2 in 1985 rather points towards an exceptional year, in terms of climatological factors, than a sudden expansion of the root zone. It can also be observed from Fig. 3a that the runoff coefficient was relatively low for 1985, suggesting either increased evaporation or a storage change. A combination of a relatively long period of low rainfall amounts and high potential evaporation, as can be noted by the relatively high mean annual potential evaporation on top of Fig. 4b, may have led to a high demand in 1985. Parts of the vegetation may not have survived these high-demand conditions due to insufficient access to water, explaining the dip in $S_{R,1yr}$ for the following year, which is also in agreement with reduced growth rates of trees after droughts as observed by for example Bréda et al. (2006). The hydrographs of 1984–1985 (Fig. 6a) and 1986–1987 (Fig. 6b) also show that July–August 1985 was exceptionally dry, whereas the next year in August 1986 the catchment seems to have increased peak flows. This either points towards an actual low storage capacity due to contraction of the roots during the dry summer or a low need of the system to use the existing capacity, for instance to recover other vital aspects of the system.

Nevertheless, Hubbard Brook WS2 does not show a clear signal of reduced root-zone storage, followed by a gradual regrowth. Here, the forest was removed in a whole-tree harvest in winter 1983–1984, followed by natural regrowth. The summers of 1984 and 1985 were very dry summers, as also reflected by the high values of $S_{R,1yr}$. The young system had already developed enough roots before these dry periods to have access to a sufficiently large water volume to survive this summer. This is plausible, as the period of the highest deficit occurred in mid-July and lasted until approximately the end of September, thus long after the beginning of the growing season, allowing enough time for an initial growth and development of young roots from April until mid-July. In addition, the composition of the new forest differed from the old forest, with more pin cherry (*Prunus pensylvanica*) and paper birch (*Betula papyrifera*). This supports the statements of a quick regeneration as these species have a high growth rate and reach canopy closure in a few years. Furthermore, the forest was not either treated with herbicides (Hubbard Brook WS2) or burned (HJ Andrews WS1), leaving enough low shrubs and herbs to maintain some level of transpiration (Hughes and Fahey, 1991; Martin, 1988). It can thus be argued, similar to Li et al. (2007), that the remaining vegetation experienced less competition and could increase root water uptake efficiency and transpiration per unit leaf area. This is in agreement with Hughes and Fahey (1991), who also stated that several species benefited from the removal of canopies and newly available resources in this catchment. Lastly, several other authors related the absence of a clear change in hydrological dynamics to the severe soil disturbance in this catchment (Hornbeck et al., 1997; Johnson et al., 1991). These disturbances lead to extra compaction, whereas at the same time species were changing, effectively masking any changes in runoff dynamics.

5.3 Process understanding – trend analysis and change in hydrological regimes

The found recovery periods correspond to recovery timescales for forest systems as reported in other studies (e.g. Brown et al., 2005; Hornbeck et al., 2014; Elliott et al., 2016) which found that catchments reach a new equilibrium with a similar timescale as reported here, but in this case with the direct link to the parameter describing the catchment-scale root-zone storage capacity. The timescales are also in agreement with regression models to predict water yield after logging of Douglass (1983), who assumed a duration of water yield increases of 12 years for coniferous catchments.

The timescales found here are around 10 years (5–13 years for the catchments under consideration), but will probably depend on climatic factors and vegetation type. HJ Andrews WS1 has a recovery (6–9 years) slightly shorter compared to Hubbard Brook WS2 (10–13 years), which could depend on the different climatological conditions of the catchments. Nevertheless, it could also be argued that the spraying of herbicides had an especially strong impact on the recovery of vegetation in Hubbard Brook WS2, as the Hubbard Brook WS5 does not show such a distinct recovery signal.

5.4 Time-variant model formulation

It was found that a time-dynamic formulation of $S_{u,max}$ merely improved the high and peak flow signatures for HJ Andrews WS1. Other authors also suggested previously (e.g. de Boer-Euser et al., 2016; Euser et al., 2015; Oudin et al., 2004) that the root-zone storage affects mostly the fast-responding components of the system, by providing a buffer to storm response. Fulfilling its function as a storage reservoir for plant-available water, modelled transpiration is significantly reduced post-deforestation, which in turn results in increased runoff coefficients (cf. Gao et al., 2014), which have been frequently reported for post-deforestation periods by earlier studies (e.g. Hornbeck et al., 2014; Rothacher, 1970; Swift and Swank, 1981)

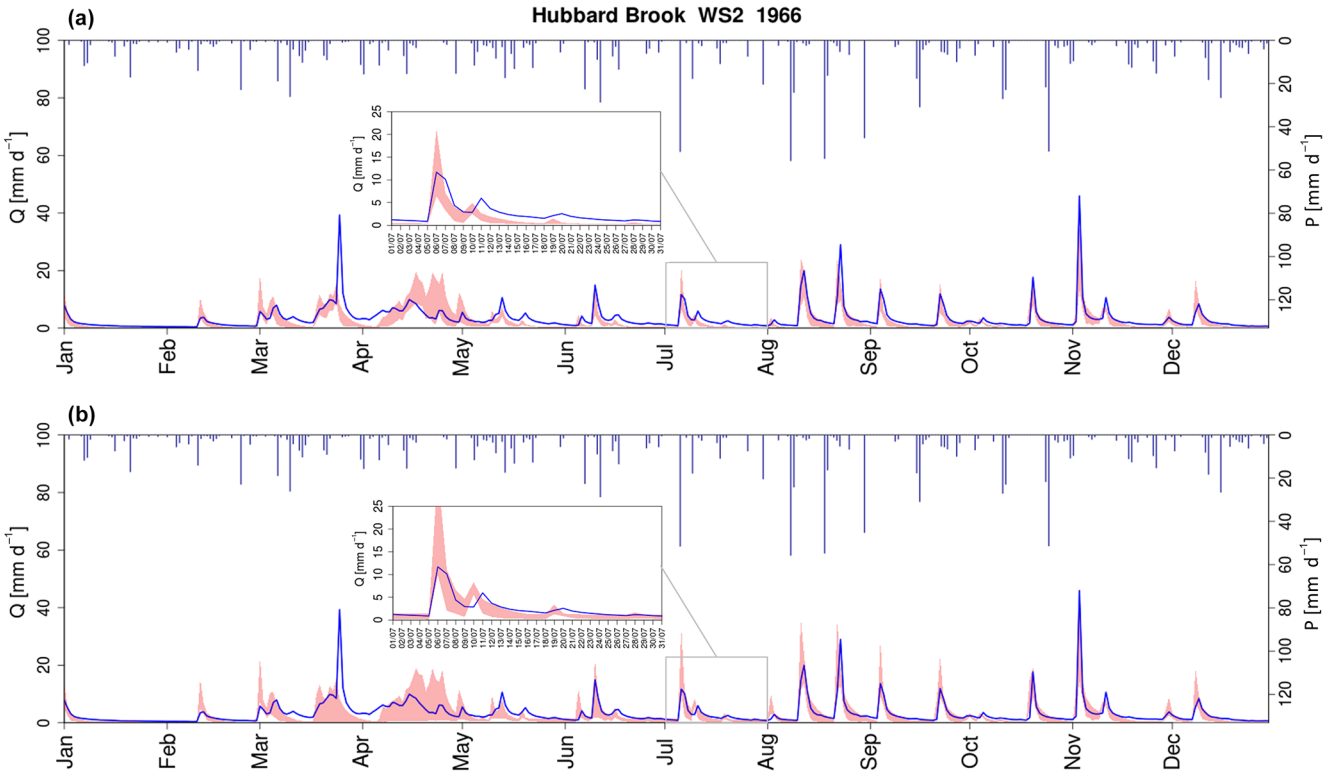

Figure 10. Hydrograph of Hubbard Brook WS2 with the observed discharge (blue) and the modelled discharge represented by the 5/95 % uncertainty intervals (red), obtained with **(a)** a constant representation of the root-zone storage capacity $S_{u,\max}$ and **(b)** a time-varying representation of the root-zone storage capacity $S_{u,\max}$. Blue bars indicate precipitation.

Nevertheless, signatures considering the peak flows did not improve for the Hubbard Brook catchments. Apparently, the model with a constant, and thus higher, $S_{u,\max}$ stored water in the root zone, reducing recharge to the groundwater reservoir that maintains the lower flows and buffering more water, reducing the peaks. This can also be clearly seen from the hydrographs (Fig. 10), where the later part of the recession in the late-summer months is much better captured by the time-dynamic model. Nevertheless, the peaks are too high for the time-dynamic model, which here is linked to an insufficient representation of snow-related processes, as can be seen from the hydrograph (April–May) as well, and possibly by an inadequate interception growth function, both leading to too high amounts of effective precipitation entering the root zone. An adjustment of these processes would have resulted in less infiltration and a smaller root-zone storage capacity.

It was acknowledged previously by several authors that certain model parameters may need time-dynamic formulations, like Waichler et al. (2005) with time-dynamic formulations of leaf area index and overstore height for the DHSVM model. In addition, Westra et al. (2014) captured long-term dynamics in the storage parameter of the GR4J model with a trend correction, in fact leading to a similar model behaviour to the Weibull growth function in this study. Nevertheless, they only hypothesized about the actual hydrological reasons for this, which aimed at the changing number of farmer dams in the catchment. The results presented here indicate that vegetation, and especially root-zone dynamics, has a strong impact on the long term non-stationarity of model parameters. The simple Weibull equation can be used as an extra equation in conceptual hydrological models to more closely reflect the dynamics of vegetation. The additional growth parameters may be left for calibration, but can also be estimated from simple water-balance-based estimations of the root-zone storage. In this way, the extra parameters should not add any uncertainty to the model outcomes.

5.5 General limitations

The results presented here depend on the quality of the data and several assumptions made in the calculations. A limiting factor is that the potential evaporation is determined from temperature only, leading to values that may be relatively low and water balances that may not close completely. Generally, this would lead to a discrepancy between the modelled $S_{u,\max}$, where potential evaporation is directly used, and the water-balance estimates of S_R. The models will probably generate higher root-zone storages in order to compensate for

the rather low potential evaporation. This can also be noted when looking at Fig. 4 for several models.

In addition, the assumption that the water balance closes in the 2-year periods under consideration may often be violated in reality. It can be argued that the estimated transpiration for the calculation of S_R represents an upper boundary, when storage changes are ignored. This would lead to estimates of S_R that may be lower than presented here. Nevertheless, attempts with 5-year water balances to reduce the influence of storage changes (see Fig. S9), showed that similar patterns were obtained. Values here were slightly lower due to more averaging in the estimation of the transpiration by the longer time period used for the water balance. Nevertheless, a strong decrease after deforestation and gradual recovery can still be observed.

The issues raised here can be fully avoided when, instead of a water-balance-based estimation of the transpiration, remote sensing products are used to estimate the transpiration, similar to Wang-Erlandsson et al. (2016). However, water-balance-based estimates may provide a rather quick solution.

The transpiration estimates were also only corrected for interception evaporation, thus assuming a negligible amount of soil evaporation. Making this additional separation is typically not warranted by the available data and would result in additional uncertainty. The transpiration estimates presented here merely represent an upper limit of transpiration and will be lower in reality due to soil evaporation. Thus, the values for $S_{R,1yr}$ may expected to be lower in reality as well.

6 Conclusions

In this study, three deforested catchments (HJ Andrews WS1, Hubbard Brook WS2 and WS5) were investigated to assess the dynamic character of root-zone storage capacities using water balance, trend analysis, four different hydrological models and one modified model version. Root-zone storage capacities were estimated based on a simple water balance approach. Results demonstrate a good correspondence between water-balance-derived root-zone storage capacities and values obtained by a 2-year moving window calibration of four distinct hydrological models.

There are significant changes in root-zone storage capacity after deforestation, which were detected by both a water-balance-based method and the calibration of hydrological models in two of the three catchments. More specifically, root-zone storage capacities showed, for HJ Andrews WS1 and Hubbard Brook WS2, a sharp decrease in root-zone storage capacities immediately after deforestation with a gradual recovery towards a new equilibrium. This could to a large extent explain post-treatment changes to the hydrological regime. These signals were however not clearly observed for Hubbard Brook WS5, probably due to soil disturbance, a new vegetation composition and a climatologically exceptional year. Nevertheless, trend analysis showed significant differences for all three catchments with their corresponding, undisturbed reference watersheds. Based on this, recovery times were estimated to be between 5 and 13 years for the three catchments under consideration.

These findings underline the fact that root-zone storage capacities in hydrological models, which are more often than not treated as constant in time, may need time-dynamic formulations with reductions after logging and gradual regrowth afterwards. Therefore, one of the models was subsequently formulated with a time-dynamic description of root-zone storage capacity. Particularly under climatic conditions with pronounced seasonality and phase shifts between precipitation and evaporation, this resulted in improvements in model performance as evaluated by 28 hydrological signatures.

Even though this more complex system behaviour may lead to extra unknown growth parameters, it has been shown here that a simple equation, reflecting the long-term growth of the system, can already suffice for a time-dynamic estimation of this crucial hydrological parameter. Therefore, this study clearly shows that observed changes in runoff characteristics after land-cover changes can be linked to relatively simple time-dynamic formulations of vegetation-related model parameters.

7 Data availability

The used input data for this research was obtained from the databases of the Hubbard Brook Experimental Forest and the HJ Andrews Experimental Forest. Time series of discharge (Campbell, 2014a; Johnson and Rothacher, 2016), precipitation (Campbell, 2014b; Daly and McKee, 2016) and temperature (Campbell, 2014c, 2014d; Daly and McKee, 2016) served as input data for the hydrological models and the water-balance estimates of root-zone storage capacities. The results of this research can be accessed through the spatial information platform of the EU-funded project Switch-on, named BYOD ("Browse your open datasets", http://www.water-switch-on.eu/sip-webclient/byod/#/map). The water-balance estimates of SR are here available for HJ Andrews WS1 (http://dl-ng003.xtr.deltares.nl/data/modelled_root_zone_storage_capacities_hj_andrews1/), Hubbard Brook WS2 (http://dl-ng003.xtr.deltares.nl/data/modelled_root_zone_storage_capacities_hubbard_brook/) and Hubbard Brook WS5 (http://dl-ng003.xtr.deltares.nl/data/modelled_root_zone_storage_capacities_hubbard_brook_ws5/). The model results for FLEX, HYPE, TUW and HYPE are also accessible through this portal, combined in one dataset for HJ Andrews WS1 (http://www.water-switch-on.eu/sip-webclient/byod/#/resource/12064), Hubbard Brook WS2 (http://www.water-switch-on.eu/sip-webclient/byod/#/resource/12065) and Hubbard Brook WS5 (http://www.water-switch-on.eu/sip-webclient/byod/#/resource/12066).

The Supplement related to this article is available online at doi:10.5194/hess-20-4775-2016-supplement.

Acknowledgements. We would like to acknowledge the European Commission FP7 funded research project "Sharing Water-related Information to Tackle Changes in the Hydrosphere – for Operational Needs" (SWITCH-ON, grant agreement number 603587), as this study was conducted within the context of SWITCH-ON as an example of scientific potential when using open data for collaborative research in hydrology.

Open Data were provided by the Hubbard Brook Ecosystem Study (HBES), which is a collaborative effort at the Hubbard Brook Experimental Forest which is operated and maintained by the USDA Forest Service Northern Research Station, Newtown Square, PA, USA.

Open Data were provided by the HJ Andrews Experimental Forest research program, funded by the National Science Foundation's Long-Term Ecological Research Program (DEB 08-23380), US Forest Service Pacific Northwest Research Station, and Oregon State University.

Edited by: F. Fenicia
Reviewed by: A. Ducharne and two anonymous referees

References

Alila, Y., Kuraś, P. K., Schnorbus, M., and Hudson, R.: Forests and floods: A new paradigm sheds light on age-old controversies, Water Resour. Res., 45, W08416, doi:10.1029/2008WR007207, 2009.

Allen, C. D., Macalady, A. K., Chenchouni, H., Bachelet, D., McDowell, N., Vennetier, M., Kitzberger, T., Rigling, A., Breshears, D. D., Hogg, E. H., Gonzalez, P., Fensham, R., Zhang, Z., Castro, J., Demidova, N., Lim, J.-H., Allard, G., Running, S. W., Semerci, A., and Cobb, N.: A global overview of drought and heat-induced tree mortality reveals emerging climate change risks for forests, Forest Ecol. Manage., 259, 660–684, doi:0.1016/j.foreco.2009.09.001, 2010.

Allen, R. G., Pereira, L. S., Raes, D., and Smith, M.: Crop evapotranspiration-Guidelines for computing crop water requirements-FAO Irrigation and drainage paper 56, FAO, Rome, 300, D05109, 1998.

Allison, G. B., Cook, P. G., Barnett, S. R., Walker, G. R., Jolly, I. D., and Hughes, M. W.: Land clearance and river salinisation in the western Murray Basin, Australia, J. Hydrol., 119, 1–20, doi:10.1016/0022-1694(90)90030-2, 1990.

Andersson, L. and Arheimer, B.: Consequences of changed wetness on riverine nitrogen – human impact on retention vs. natural climatic variability, Reg. Environ. Change, 2, 93–105, doi:10.1007/s101130100024, 2001.

Andréassian, V.: Waters and forests: from historical controversy to scientific debate, J. Hydrol., 291, 1–27, doi:10.1016/j.jhydrol.2003.12.015, 2004.

Bathurst, J. C., Ewen, J., Parkin, G., O'Connell, P. E., and Cooper, J. D.: Validation of catchment models for predicting land-use and climate change impacts, 3. Blind validation for internal and outlet responses, J. Hydrol., 287, 74–94, doi:10.1016/j.jhydrol.2003.09.021, 2004.

Bergström, S.: Development and application of a conceptual runoff model for Scandinavian catchments, SMHI Reports RHO, Norrköping, 1976.

Bergström, S.: The HBV model: Its structure and applications, Swedish Meteorological and Hydrological Institute, 1992.

Black, P. E.: Watershed functions1, JAWRA Journal of the American Water Resources Association, 33, 1–11, doi:10.1111/j.1752-1688.1997.tb04077.x, 1997.

Bosch, J. M. and Hewlett, J. D.: A review of catchment experiments to determine the effect of vegetation changes on water yield and evapotranspiration, J. Hydrol., 55, 3–23, doi:10.1016/0022-1694(82)90117-2, 1982.

Boyle, D. P.: Multicriteria calibration of hydrologic models, 2001.

Brath, A., Montanari, A., and Moretti, G.: Assessing the effect on flood frequency of land use change via hydrological simulation (with uncertainty), J. Hydrol., 324, 141–153, doi:10.1016/j.jhydrol.2005.10.001, 2006.

Bréda, N., Huc, R., Granier, A., and Dreyer, E.: Temperate forest trees and stands under severe drought: a review of ecophysiological responses, adaptation processes and long-term consequences, Ann. Forest Sci., 63, 625–644, 2006.

Breuer, L., Eckhardt, K., and Frede, H.-G.: Plant parameter values for models in temperate climates, Ecol. Modell., 169, 237–293, doi:10.1016/S0304-3800(03)00274-6, 2003.

Brown, A. E., Zhang, L., McMahon, T. A., Western, A. W., and Vertessy, R. A.: A review of paired catchment studies for determining changes in water yield resulting from alterations in vegetation, J. Hydrol., 310, 28–61, doi:10.1016/j.jhydrol.2004.12.010, 2005.

Brunner, I., Herzog, C., Dawes, M. A., Arend, M., and Sperisen, C.: How tree roots respond to drought, Front. Plant Sci., 6, 547, doi:10.3389/fpls.2015.00547, 2015.

Brunner, P. and Simmons, C. T.: HydroGeoSphere: A Fully Integrated, Physically Based Hydrological Model, Ground Water, 50, 170–176, doi:10.1111/j.1745-6584.2011.00882.x, 2012.

Campbell, J.: Hubbard Brook Experimental Forest (USDA Forest Service): Daily Streamflow by Watershed, 1956–present, available at: http://www.hubbardbrook.org/data/dataset.php?id=2 (last access: 29 November 2016), 2014a.

Campbell, J.: Hubbard Brook Experimental Forest (US Forest Service): Daily Precipitation Standard Rain Gage Measurements, 1956–present, available at: http://www.hubbardbrook.org/data/dataset.php?id=13 (last access: 29 November 2016), 2014b.

Campbell, J.: Hubbard Brook Experimental Forest (USDA Forest Service): Daily Maximum and Minimum Temperature Records, 1955–present, available at: http://www.hubbardbrook.org/data/dataset.php?id=59, 2014c.

Campbell, J.: Hubbard Brook Experimental Forest (USDA Forest Service): Daily Mean Temperature Data, 1955–present, available at: http://www.hubbardbrook.org/data/dataset.php?id=58, 2014d.

Campbell, J. L., Bailey, A. S., Eagar, C., Green, M. B., and Battles, J. J.: Vegetation treatments and hydrologic responses at the Hubbard Brook Experimental Forest, New Hampshire, in: Long-term silvicultural & ecological studies: Results for science and

management, Yale University, Global Institute of Sustainable Forestry, Research Paper 013, 2, 011–019, 2013.

Camporese, M., Daly, E., and Paniconi, C.: Catchment-scale Richards equation-based modeling of evapotranspiration via boundary condition switching and root water uptake schemes, Water Resour. Res., 51, 5756–5771, doi:10.1002/2015WR017139, 2015.

Cassiani, G., Boaga, J., Vanella, D., Perri, M. T., and Consoli, S.: Monitoring and modelling of soil-plant interactions: the joint use of ERT, sap flow and eddy covariance data to characterize the volume of an orange tree root zone, Hydrol. Earth Syst. Sci., 19, 2213–2225, doi:10.5194/hess-19-2213-2015, 2015.

Ceola, S., Arheimer, B., Baratti, E., Blöschl, G., Capell, R., Castellarin, A., Freer, J., Han, D., Hrachowitz, M., Hundecha, Y., Hutton, C., Lindström, G., Montanari, A., Nijzink, R., Parajka, J., Toth, E., Viglione, A., and Wagener, T.: Virtual laboratories: new opportunities for collaborative water science, Hydrol. Earth Syst. Sci., 19, 2101–2117, doi:10.5194/hess-19-2101-2015, 2015.

Dahlgren, R. A. and Driscoll, C. T.: The effects of whole-tree clear-cutting on soil processes at the Hubbard Brook Experimental Forest, New Hampshire, USA, Plant Soil, 158, 239–262, doi:10.1007/BF00009499, 1994.

Daly, C. and McKee, W.: Meteorological data from benchmark stations at the Andrews Experimental Forest, 1957 to present, Long-Term Ecological Research, Forest Science Data Bank, available at: http://andrewsforest.oregonstate.edu/data/abstract.cfm?dbcode=MS001, last access: 29 November 2016.

de Boer-Euser, T., McMillan, H. K., Hrachowitz, M., Winsemius, H. C., and Savenije, H. H. G.: Influence of soil and climate on root zone storage capacity, Water Resour. Res., 52, 2009–2024, doi:10.1002/2015WR018115, 2016.

Donohue, R. J., Roderick, M. L., and McVicar, T. R.: On the importance of including vegetation dynamics in Budyko's hydrological model, Hydrol. Earth Syst. Sci., 11, 983–995, doi:10.5194/hess-11-983-2007, 2007.

Donohue, R. J., Roderick, M. L., and McVicar, T. R.: Roots, storms and soil pores: Incorporating key ecohydrological processes into Budyko's hydrological model, J. Hydrol., 436–437, 35–50, doi:10.1016/j.jhydrol.2012.02.033, 2012.

Douglass, J. E.: The potential for water yield augmentation from forest management in the eastern united states1, JAWRA Journal of the American Water Resources Association, 19, 351–358, doi:10.1111/j.1752-1688.1983.tb04592.x, 1983.

Du, E., Link, T. E., Wei, L., and Marshall, J. D.: Evaluating hydrologic effects of spatial and temporal patterns of forest canopy change using numerical modelling, Hydrol. Process., 30, 217–231, doi:10.1002/hyp.10591, 2016.

Dyrness, C.: Hydrologic properties of soils on three small watersheds in the western Cascades of Oregon, Res. Note PNW-111, US Department of Agriculture, Forest Service, Pacific Northwest Forest and Range Experiment Station: Portland, OR, 17, 1969.

Eagleson, P. S.: Climate, soil, and vegetation: 3. A simplified model of soil moisture movement in the liquid phase, Water Resour. Res., 14, 722–730, doi:10.1029/WR014i005p00722, 1978.

Eagleson, P. S.: Ecological optimality in water-limited natural soil-vegetation systems: 1. Theory and hypothesis, Water Resour. Res., 18, 325–340, doi:10.1029/WR018i002p00325, 1982.

Ehret, U., Gupta, H. V., Sivapalan, M., Weijs, S. V., Schymanski, S. J., Blöschl, G., Gelfan, A. N., Harman, C., Kleidon, A., Bogaard, T. A., Wang, D., Wagener, T., Scherer, U., Zehe, E., Bierkens, M. F. P., Di Baldassarre, G., Parajka, J., van Beek, L. P. H., van Griensven, A., Westhoff, M. C., and Winsemius, H. C.: Advancing catchment hydrology to deal with predictions under change, Hydrol. Earth Syst. Sci., 18, 649–671, doi:10.5194/hess-18-649-2014, 2014.

Elliott, K. J., Caldwell, P. V., Brantley, S. T., Miniat, C. F., Vose, J. M., and Swank, W. T.: Water yield following forest-grass-forest transitions, Hydrol. Earth Syst. Sci. Discuss., doi:10.5194/hess-2016-548, in review, 2016.

Euser, T., Winsemius, H. C., Hrachowitz, M., Fenicia, F., Uhlenbrook, S., and Savenije, H. H. G.: A framework to assess the realism of model structures using hydrological signatures, Hydrol. Earth Syst. Sci., 17, 1893–1912, doi:10.5194/hess-17-1893-2013, 2013.

Euser, T., Hrachowitz, M., Winsemius, H. C., and Savenije, H. H. G.: The effect of forcing and landscape distribution on performance and consistency of model structures, Hydrol. Process., 29, 3727–3743, doi:10.1002/hyp.10445, 2015.

Fatichi, S., Pappas, C., and Ivanov, V. Y.: Modeling plant–water interactions: an ecohydrological overview from the cell to the global scale, Wiley Interdisciplinary Reviews: Water, 3, 327–368, doi:10.1002/wat2.1125, 2016.

Feddes, R. A., Kowalik, P. J., and Zaradny, H.: Simulation of field water use and crop yield, Centre for Agricultural Publishing and Documentation, 1978.

Federer, A. C., Flynn, L. D., Martin, W. C., Hornbeck, J. W., and Pierce, R. S.: Thirty years of hydrometeorologic data at the Hubbard Brook Experiment Forest, New Hampshire, 1990.

Fenicia, F., Savenije, H. H. G., Matgen, P., and Pfister, L.: Is the groundwater reservoir linear? Learning from data in hydrological modelling, Hydrol. Earth Syst. Sci., 10, 139–150, doi:10.5194/hess-10-139-2006, 2006.

Fenicia, F., Savenije, H. H. G., Matgen, P., and Pfister, L.: Understanding catchment behavior through stepwise model concept improvement, Water Resour. Res., 44, W01402, doi:10.1029/2006WR005563, 2008.

Fenicia, F., Savenije, H. H. G., and Avdeeva, Y.: Anomaly in the rainfall-runoff behaviour of the Meuse catchment, Climate, land-use, or land-use management?, Hydrol. Earth Syst. Sci., 13, 1727–1737, doi:10.5194/hess-13-1727-2009, 2009.

Freer, J., Beven, K., and Ambroise, B.: Bayesian Estimation of Uncertainty in Runoff Prediction and the Value of Data: An Application of the GLUE Approach, Water Resour. Res., 32, 2161–2173, doi:10.1029/95WR03723, 1996.

Gao, H., Hrachowitz, M., Schymanski, S. J., Fenicia, F., Sriwongsitanon, N., and Savenije, H. H. G.: Climate controls how ecosystems size the root zone storage capacity at catchment scale, Geophys. Res. Lett., 41, 7916–7923, doi:10.1002/2014GL061668, 2014.

Gentine, P., D'Odorico, P., Lintner, B. R., Sivandran, G., and Salvucci, G.: Interdependence of climate, soil, and vegetation as constrained by the Budyko curve, Geophys. Res. Lett., 39, L19404, doi:10.1029/2012GL053492, 2012.

Gerrits, A. M. J., Pfister, L., and Savenije, H. H. G.: Spatial and temporal variability of canopy and forest floor interception in a beech forest, Hydrol. Process., 24, 3011–3025, doi:10.1002/hyp.7712, 2010.

Gumbel, E. J.: The Return Period of Flood Flows, The Annals of Mathematical Statistics, 12, 163–190, 1941.

Gupta, H. V., Kling, H., Yilmaz, K. K., and Martinez, G. F.: Decomposition of the mean squared error and NSE performance criteria: Implications for improving hydrological modelling, J. Hydrol., 377, 80–91, doi:10.1016/j.jhydrol.2009.08.003, 2009.

Hargreaves, G. H. and Samani, Z. A.: Reference Crop Evapotranspiration from Temperature, Appl. Eng. Agr., 1, 96–99, doi:10.13031/2013.26773, 1985.

Harr, R. D., Harper, W. C., Krygier, J. T., and Hsieh, F. S.: Changes in storm hydrographs after road building and clear-cutting in the Oregon Coast Range, Water Resour. Res., 11, 436–444, doi:10.1029/WR011i003p00436, 1975.

Hornbeck, J. W., Pierce, R. S., and Federer, C. A.: Streamflow Changes after Forest Clearing in New England, Water Resour. Res., 6, 1124–1132, doi:10.1029/WR006i004p01124, 1970.

Hornbeck, J. W.: Storm flow from hardwood-forested and cleared watersheds in New Hampshire, Water Resour. Res., 9, 346–354, doi:10.1029/WR009i002p00346, 1973.

Hornbeck, J. W., Martin, C. W., and Eagar, C.: Summary of water yield experiments at Hubbard Brook Experimental Forest, New Hampshire, Can. J. Forest Res., 27, 2043–2052, doi:10.1139/x97-173, 1997.

Hornbeck, J. W., Eagar, C., Bailey, A., and Campbell, J. L.: Comparisons with results from the Hubbard Brook Experimental Forest in the Northern Appalachians, Long-Term Response of a Forest Watershed Ecosystem: Clearcutting in the Southern Appalachians, 213 pp., 2014.

Hrachowitz, M., Savenije, H. H. G., Blöschl, G., McDonnell, J. J., Sivapalan, M., Pomeroy, J. W., Arheimer, B., Blume, T., Clark, M. P., Ehret, U., Fenicia, F., Freer, J. E., Gelfan, A., Gupta, H. V., Hughes, D. A., Hut, R. W., Montanari, A., Pande, S., Tetzlaff, D., Troch, P. A., Uhlenbrook, S., Wagener, T., Winsemius, H. C., Woods, R. A., Zehe, E., and Cudennec, C.: A decade of Predictions in Ungauged Basins (PUB) – a review, Hydrol. Sci. J., 58, 1198–1255, doi:10.1080/02626667.2013.803183, 2013.

Hrachowitz, M., Fovet, O., Ruiz, L., Euser, T., Gharari, S., Nijzink, R., Freer, J., Savenije, H. H. G., and Gascuel-Odoux, C.: Process consistency in models: The importance of system signatures, expert knowledge, and process complexity, Water Resour. Res., 50, 7445–7469, doi:10.1002/2014WR015484, 2014.

Hughes, J. W. and Fahey, T. J.: Colonization Dynamics of Herbs and Shrubs in a Disturbed Northern Hardwood Forest, J. Ecol., 79, 605–616, doi:10.2307/2260656, 1991.

Ivanov, V. Y., Bras, R. L., and Vivoni, E. R.: Vegetation-hydrology dynamics in complex terrain of semiarid areas: 1. A mechanistic approach to modeling dynamic feedbacks, Water Resour. Res., 44, W03429, doi:10.1029/2006WR005588, 2008.

Jobbágy, E. G. and Jackson, R. B.: Groundwater use and salinization with grassland afforestation, Glob. Change Biol., 10, 1299–1312, doi:10.1111/j.1365-2486.2004.00806.x, 2004.

Johnson, C. E., Johnson, A. H., Huntington, T. G., and Siccama, T. G.: Whole-Tree Clear-Cutting Effects on Soil Horizons and Organic-Matter Pools, Soil Sci. Soc. Am. J., 55, 497–502, doi:10.2136/sssaj1991.03615995005500020034x, 1991.

Johnson, S. and Rothacher, J.: Stream discharge in gaged watersheds at the Andrews Experimental Forest, 1949 to present, Long-Term Ecological Research, Forest Science Data Bank, Forest Science Data Bank, http://andrewsforest.oregonstate.edu/data/abstract.cfm?dbcode=HF004, last access: 29 November 2016.

Jones, J. A. and Grant, G. E.: Peak Flow Responses to Clear-Cutting and Roads in Small and Large Basins, Western Cascades, Oregon, Water Resour. Res., 32, 959–974, doi:10.1029/95WR03493, 1996.

Jones, J. A. and Post, D. A.: Seasonal and successional streamflow response to forest cutting and regrowth in the northwest and eastern United States, Water Resour. Res., 40, W05203, doi:10.1029/2003WR002952, 2004.

Jothityangkoon, C., Sivapalan, M., and Farmer, D. L.: Process controls of water balance variability in a large semi-arid catchment: downward approach to hydrological model development, J. Hydrol., 254, 174–198, doi:10.1016/S0022-1694(01)00496-6, 2001.

Kleidon, A.: Global Datasets of Rooting Zone Depth Inferred from Inverse Methods, J. Climate, 17, 2714–2722, 2004.

Kuczera, G.: Prediction of water yield reductions following a bushfire in ash-mixed species eucalypt forest, J. Hydrol., 94, 215–236, doi:10.1016/0022-1694(87)90054-0, 1987.

Laio, F., Porporato, A., Ridolfi, L., and Rodriguez-Iturbe, I.: Plants in water-controlled ecosystems: active role in hydrologic processes and response to water stress: II. Probabilistic soil moisture dynamics, Adv. Water Resour., 24, 707–723, doi:10.1016/S0309-1708(01)00005-7, 2001.

Legesse, D., Vallet-Coulomb, C., and Gasse, F.: Hydrological response of a catchment to climate and land use changes in Tropical Africa: case study South Central Ethiopia, J. Hydrol., 275, 67–85, doi:10.1016/S0022-1694(03)00019-2, 2003.

Li, K. Y., Coe, M. T., Ramankutty, N., and Jong, R. D.: Modeling the hydrological impact of land-use change in West Africa, J. Hydrol., 337, 258–268, doi:10.1016/j.jhydrol.2007.01.038, 2007.

Liancourt, P., Sharkhuu, A., Ariuntsetseg, L., Boldgiv, B., Helliker, B. R., Plante, A. F., Petraitis, P. S., and Casper, B. B.: Temporal and spatial variation in how vegetation alters the soil moisture response to climate manipulation, Plant Soil, 351, 249–261, doi:10.1007/s11104-011-0956-y, 2012.

Likens, G. E., Bormann, F. H., Johnson, N. M., Fisher, D. W., and Pierce, R. S.: Effects of Forest Cutting and Herbicide Treatment on Nutrient Budgets in the Hubbard Brook Watershed-Ecosystem, Ecol. Monogr., 40, 23–47, doi:10.2307/1942440, 1970.

Likens, G. E.: Biogeochemistry of a forested ecosystem, Springer, New York, 2013.

Lindström, G., Pers, C., Rosberg, J., Strömqvist, J., and Arheimer, B.: Development and testing of the HYPE (Hydrological Predictions for the Environment) water quality model for different spatial scales, Hydrol. Res., 41, 295–319, doi:10.2166/nh.2010.007, 2010.

Mahe, G., Paturel, J.-E., Servat, E., Conway, D., and Dezetter, A.: The impact of land use change on soil water holding capacity and river flow modelling in the Nakambe River, Burkina-Faso, J. Hydrol., 300, 33–43, doi:10.1016/j.jhydrol.2004.04.028, 2005.

Martin, C. W.: Soil disturbance by logging in New England–review and management recommendations, Northern J. Appl. Forest., 5, 30–34, 1988.

Martin, C. W., Hornbeck, J. W., Likens, G. E., and Buso, D. C.: Impacts of intensive harvesting on hydrology and nutrient dynamics

of northern hardwood forests, Can. J. Fish. Aquat. Sci., 57, 19–29, doi:10.1139/f00-106, 2000.

McDowell, N., Pockman, W. T., Allen, C. D., Breshears, D. D., Cobb, N., Kolb, T., Plaut, J., Sperry, J., West, A., Williams, D. G., and Yepez, E. A.: Mechanisms of plant survival and mortality during drought: why do some plants survive while others succumb to drought?, New Phytol., 178, 719–739, doi:10.1111/j.1469-8137.2008.02436.x, 2008.

Mencuccini, M.: The ecological significance of long-distance water transport: short-term regulation, long-term acclimation and the hydraulic costs of stature across plant life forms, Plant Cell Environ., 26, 163–182, doi:10.1046/j.1365-3040.2003.00991.x, 2003.

Milly, P. C. D.: Climate, soil water storage, and the average annual water balance, Water Resour. Res., 30, 2143–2156, doi:10.1029/94WR00586, 1994.

Milly, P. C. D. and Dunne, K. A.: Sensitivity of the Global Water Cycle to the Water-Holding Capacity of Land, J. Climate, 7, 506–526, 1994.

Montanari, A. and Toth, E.: Calibration of hydrological models in the spectral domain: An opportunity for scarcely gauged basins?, Water Resour. Res., 43, W05434, doi:10.1029/2006WR005184, 2007.

Montanari, A., Young, G., Savenije, H. H. G., Hughes, D., Wagener, T., Ren, L. L., Koutsoyiannis, D., Cudennec, C., Toth, E., Grimaldi, S., Blöschl, G., Sivapalan, M., Beven, K., Gupta, H., Hipsey, M., Schaefli, B., Arheimer, B., Boegh, E., Schymanski, S. J., Di Baldassarre, G., Yu, B., Hubert, P., Huang, Y., Schumann, A., Post, D. A., Srinivasan, V., Harman, C., Thompson, S., Rogger, M., Viglione, A., McMillan, H., Characklis, G., Pang, Z., and Belyaev, V.: "Panta Rhei – Everything Flows": Change in hydrology and society – The IAHS Scientific Decade 2013–2022, Hydrol. Sci. J., 58, 1256–1275, doi:10.1080/02626667.2013.809088, 2013.

Mou, P., Fahey, T. J., and Hughes, J. W.: Effects of Soil Disturbance on Vegetation Recovery and Nutrient Accumulation Following Whole-Tree Harvest of a Northern Hardwood Ecosystem, J. Appl. Ecol., 30, 661–675, doi:10.2307/2404245, 1993.

Nash, J. E. and Sutcliffe, J. V.: River flow forecasting through conceptual models part I – A discussion of principles, J. Hydrol., 10, 282–290, doi:10.1016/0022-1694(70)90255-6, 1970.

Nijzink, R. C., Samaniego, L., Mai, J., Kumar, R., Thober, S., Zink, M., Schäfer, D., Savenije, H. H. G., and Hrachowitz, M.: The importance of topography-controlled sub-grid process heterogeneity and semi-quantitative prior constraints in distributed hydrological models, Hydrol. Earth Syst. Sci., 20, 1151–1176, doi:10.5194/hess-20-1151-2016, 2016.

Nobel, P. S. and Cui, M.: Hydraulic Conductances of the Soil, the Root-Soil Air Gap, and the Root: Changes for Desert Succulents in Drying Soil, J. Exp. Bot., 43, 319–326, doi:10.1093/jxb/43.3.319, 1992.

North, G. B. and Nobel, P. S.: Drought-induced changes in hydraulic conductivity and structure in roots of Ferocactus acanthodes and Opuntia ficus-indica, New Phytol., 120, 9–19, doi:10.1111/j.1469-8137.1992.tb01053.x, 1992.

Onstad, C. A. and Jamieson, D. G.: Modeling the Effect of Land Use Modifications on Runoff, Water Resour. Res., 6, 1287–1295, doi:10.1029/WR006i005p01287, 1970.

Oudin, L., Andréassian, V., Perrin, C., and Anctil, F.: Locating the sources of low-pass behavior within rainfall-runoff models, Water Resour. Res., 40, W11101, doi:10.1029/2004WR003291, 2004.

Parajka, J., Merz, R., and Blöschl, G.: Uncertainty and multiple objective calibration in regional water balance modelling: case study in 320 Austrian catchments, Hydrol. Process., 21, 435–446, doi:10.1002/hyp.6253, 2007.

Patric, J. H. and Reinhart, K. G.: Hydrologic Effects of Deforesting Two Mountain Watersheds in West Virginia, Water Resour. Res., 7, 1182–1188, doi:10.1029/WR007i005p01182, 1971.

Perrin, C., Michel, C., and Andréassian, V.: Improvement of a parsimonious model for streamflow simulation, J. Hydrol., 279, 275–289, doi:10.1016/S0022-1694(03)00225-7, 2003.

Porporato, A., Daly, E., Rodriguez, x, Iturbe, I., and Associate Editor: William, F. F.: Soil Water Balance and Ecosystem Response to Climate Change, Am. Nat., 164, 625–632, doi:10.1086/424970, 2004.

Refsgaard, J. C. and Storm, B.: MIKE SHE, in: Computer Models of Watershed Hydrology, edited by: Singh, V. J., Water Resour. Publ., Littleton, Colorado, 1995.

Reynolds, J. F., Kemp, P. R., and Tenhunen, J. D.: Effects of long-term rainfall variability on evapotranspiration and soil water distribution in the Chihuahuan Desert: A modeling analysis, Plant Ecol., 150, 145–159, doi:10.1023/a:1026530522612, 2000.

Rodriguez-Iturbe, I.: Ecohydrology: A hydrologic perspective of climate-soil-vegetation dynamies, Water Resour. Res., 36, 3–9, doi:10.1029/1999WR900210, 2000.

Rodriguez-Iturbe, I., D'Odorico, P., Laio, F., Ridolfi, L., and Tamea, S.: Challenges in humid land ecohydrology: Interactions of water table and unsaturated zone with climate, soil, and vegetation, Water Resour. Res., 43, W09301, doi:10.1029/2007WR006073, 2007.

Rood, S. B., Braatne, J. H., and Hughes, F. M. R.: Ecophysiology of riparian cottonwoods: stream flow dependency, water relations and restoration, Tree Physiol., 23, 1113–1124, doi:10.1093/treephys/23.16.1113, 2003.

Rothacher, J.: Streamflow from small watersheds on the western slope of the Cascade Range of Oregon, Water Resour. Res., 1, 125–134, doi:10.1029/WR001i001p00125, 1965.

Rothacher, J., Dyrness, C. T., Fredriksen, R. L., Forest, P. N., and Station, R. E.: Hydrologic and related characteristics of three small watersheds in the Oregon Cascades, Pacific Northwest Forest and Range Experiment Station, US Dept. of Agriculture, 1967.

Rothacher, J.: Increases in Water Yield Following Clear-Cut Logging in the Pacific Northwest, Water Resour. Res., 6, 653–658, doi:10.1029/WR006i002p00653, 1970.

Schenk, H. J. and Jackson, R. B.: Rooting depths, lateral root spreads and below-ground/above-ground allometries of plants in water-limited ecosystems, J. Ecol., 90, 480–494, doi:10.1046/j.1365-2745.2002.00682.x, 2002.

Schoups, G., Hopmans, J. W., Young, C. A., Vrugt, J. A., and Wallender, W. W.: Multi-criteria optimization of a regional spatially-distributed subsurface water flow model, J. Hydrol., 311, 20–48, doi:10.1016/j.jhydrol.2005.01.001, 2005.

Schymanski, S. J., Sivapalan, M., Roderick, M. L., Beringer, J., and Hutley, L. B.: An optimality-based model of the coupled soil

moisture and root dynamics, Hydrol. Earth Syst. Sci., 12, 913–932, doi:10.5194/hess-12-913-2008, 2008.

Seibert, J. and McDonnell, J. J.: Land-cover impacts on streamflow: a change-detection modelling approach that incorporates parameter uncertainty, Hydrol. Sci. J., 55, 316–332, doi:10.1080/02626661003683264, 2010.

Seibert, J., McDonnell, J. J., and Woodsmith, R. D.: Effects of wildfire on catchment runoff response: a modelling approach to detect changes in snow-dominated forested catchments, Hydrol. Res., 41, 378–390, 2010.

Seneviratne, S. I., Corti, T., Davin, E. L., Hirschi, M., Jaeger, E. B., Lehner, I., Orlowsky, B., and Teuling, A. J.: Investigating soil moisture–climate interactions in a changing climate: A review, Earth-Sci. Rev., 99, 125–161, doi:10.1016/j.earscirev.2010.02.004, 2010.

Seneviratne, S. I., Wilhelm, M., Stanelle, T., van den Hurk, B., Hagemann, S., Berg, A., Cheruy, F., Higgins, M. E., Meier, A., Brovkin, V., Claussen, M., Ducharne, A., Dufresne, J.-L., Findell, K. L., Ghattas, J., Lawrence, D. M., Malyshev, S., Rummukainen, M., and Smith, B.: Impact of soil moisture-climate feedbacks on CMIP5 projections: First results from the GLACE-CMIP5 experiment, Geophys. Res. Lett., 40, 5212–5217, doi:10.1002/grl.50956, 2013.

Shamir, E., Imam, B., Morin, E., Gupta, H. V., and Sorooshian, S.: The role of hydrograph indices in parameter estimation of rainfall–runoff models, Hydrol. Process., 19, 2187–2207, doi:10.1002/hyp.5676, 2005.

Sivapalan, M., Blöschl, G., Zhang, L., and Vertessy, R.: Downward approach to hydrological prediction, Hydrol. Process., 17, 2101–2111, doi:10.1002/hyp.1425, 2003.

Sperry, J. S., Hacke, U. G., Oren, R., and Comstock, J. P.: Water deficits and hydraulic limits to leaf water supply, Plant Cell Environ., 25, 251–263, doi:10.1046/j.0016-8025.2001.00799.x, 2002.

Swift, L. W. and Swank, W. T.: Long term responses of streamflow following clearcutting and regrowth/Réactions à long terme du débit des cours d'eau après coupe et repeuplement, Hydrological Sciences Bulletin, 26, 245–256, doi:10.1080/02626668109490884, 1981.

Teuling, A. J., Van Loon, A. F., Seneviratne, S. I., Lehner, I., Aubinet, M., Heinesch, B., Bernhofer, C., Grünwald, T., Prasse, H., and Spank, U.: Evapotranspiration amplifies European summer drought, Geophys. Res. Lett., 40, 2071–2075, doi:10.1002/grl.50495, 2013.

Troch, P. A., Martinez, G. F., Pauwels, V. R. N., Durcik, M., Sivapalan, M., Harman, C., Brooks, P. D., Gupta, H., and Huxman, T.: Climate and vegetation water use efficiency at catchment scales, Hydrol. Process., 23, 2409–2414, doi:10.1002/hyp.7358, 2009.

Troch, P. A., Lahmers, T., Meira, A., Mukherjee, R., Pedersen, J. W., Roy, T., and Valdés-Pineda, R.: Catchment coevolution: A useful framework for improving predictions of hydrological change?, Water Resour. Res., 51, 4903–4922, doi:10.1002/2015WR017032, 2015.

Tron, S., Perona, P., Gorla, L., Schwarz, M., Laio, F., and Ridolfi, L.: The signature of randomness in riparian plant root distributions, Geophys. Res. Lett., 42, 7098–7106, doi:10.1002/2015GL064857, 2015.

Vose, J. M., Miniat, C. F., Luce, C. H., Asbjornsen, H., Caldwell, P. V., Campbell, J. L., Grant, G. E., Isaak, D. J., Loheide Ii, S. P., and Sun, G.: Ecohydrological implications of drought for forests in the United States, Forest Ecol. Manage., 380, 335–345, doi:10.1016/j.foreco.2016.03.025, 2016.

Wagener, T., Sivapalan, M., Troch, P., and Woods, R.: Catchment Classification and Hydrologic Similarity, Geography Compass, 1, 901–931, 10.1111/j.1749-8198.2007.00039.x, 2007.

Waichler, S. R., Wemple, B. C., and Wigmosta, M. S.: Simulation of water balance and forest treatment effects at the H.J. Andrews Experimental Forest, Hydrol. Process., 19, 3177–3199, doi:10.1002/hyp.5841, 2005.

Wang-Erlandsson, L., Bastiaanssen, W. G. M., Gao, H., Jägermeyr, J., Senay, G. B., van Dijk, A. I. J. M., Guerschman, J. P., Keys, P. W., Gordon, L. J., and Savenije, H. H. G.: Global root zone storage capacity from satellite-based evaporation, Hydrol. Earth Syst. Sci., 20, 1459–1481, doi:10.5194/hess-20-1459-2016, 2016.

Weibull, W.: A Statistical Distribution Function of Wide Applicability, J. Appl. Mech., 18, 293–297, 1951.

Westerberg, I. K., Guerrero, J.-L., Younger, P. M., Beven, K. J., Seibert, J., Halldin, S., Freer, J. E., and Xu, C.-Y.: Calibration of hydrological models using flow-duration curves, Hydrol. Earth Syst. Sci., 15, 2205–2227, doi:10.5194/hess-15-2205-2011, 2011.

Westra, S., Thyer, M., Leonard, M., Kavetski, D., and Lambert, M.: A strategy for diagnosing and interpreting hydrological model nonstationarity, Water Resour. Res., 50, 5090–5113, doi:10.1002/2013WR014719, 2014.

Wilks, D. S.: Statistical Methods in the Atmospheric Sciences, Elsevier Science, 2005.

Yadav, M., Wagener, T., and Gupta, H.: Regionalization of constraints on expected watershed response behavior for improved predictions in ungauged basins, Adv. Water Resour., 30, 1756–1774, doi:10.1016/j.advwatres.2007.01.005, 2007.

Yilmaz, K. K., Gupta, H. V., and Wagener, T.: A process-based diagnostic approach to model evaluation: Application to the NWS distributed hydrologic model, Water Resour. Res., 44, W09417, doi:10.1029/2007WR006716, 2008.

Zhang, S., Yang, H., Yang, D., and Jayawardena, A. W.: Quantifying the effect of vegetation change on the regional water balance within the Budyko framework, Geophys. Res. Lett., 43, 1140–1148, doi:10.1002/2015GL066952, 2016.

Zhao, R.-J.: The Xinanjiang model applied in China, J. Hydrol., 135, 371–381, doi:10.1016/0022-1694(92)90096-E, 1992.